PONTIFICIA UNIVERSIDAD CATÓLICA DE CHILE
Faculty of Biological Science
Doctoral Program in Biological Science
Physiological Sciences mention

"COAGULATION FACTOR Xa PROMOTES METASTASIS THROUGH ENDOTHELIAL CELL ACTIVATION"

Thesis presented to Pontificia Universidad Católica de Chile in partial fulfillment of the requirements to qualify for the doctoral degree in Biological Sciences with a mention in Physiological Sciences

MAXIMILIANO AMADEO ARCE ARATA

Thesis director:	Dr. Gareth Owen
Thesis co-director:	Dr. Andrew Quest
Thesis committee:	Dr. Alejandro Godoy
	Dr. Julio Amigo
	Dr. Julio Tapia

JUNE 2019

DEDICATORY

To my family, friends and colleagues for their constant support and love.

ACKNOWLEDGMENTS

This study was funded by the grants issued by CONICYT, Government of Chile: Beca doctorado nacional n° 21160705, CONICYT FONDAP-15130011, Millennium Institute on Immunology & Immunotherapy IMII P09/016-F, Basal AFB 170004, FONDECYT 1140970, 1170925, 1171703, 1150744, 1161115, 15130011 and 1180241 and the Swedish Cancer Society (CAN 2017/502). We especially thanks to Dr Alejandro Godoy and Patricia Fuenzalida (PUC) for their kindly support in HUVEC obtention and cultivation. We also want to thank to Rocío Artigas, coordinator of the Biodata Core facility (ACCDiS) for her scientific support in the microarray analysis and to Tania Koning, Pamela Orellana, Lorena Lobos and Veronica Silva for their excellent support in the development of *in vivo* models in this study.

MAIN INDEX

ABBREVIATION LIST

BSA : Bovine Serum Albumin

DMEM : Dulbecco's Modified Eagle Medium

FAK : Focal Adhesion Kinase

FBS : Fetal Bovine Serum

FGF-2 : Fibroblast Growth Factor 2

FVII : Coagulation Factor VII

FVIIa : Activated Coagulation Factor VII

FX : Coagulation Factor X

FXa : Activated Coagulation Factor X

GFP : Green fluorescent Protein

HUVEC : Human Umbilical Vein Endothelial Cell

HPMEC : Human Pulmonary Microvascular Endothelial Cell

IL-1β : Interleukin 1 Beta

IMDM : Iscove's Modified Dulbecco's Medium

IOI : Integrated Optical Intensity

L : Liter

LPS : Lipopolysaccharide

M : Molar

m : meter

mRNA : Messenger RNA

min : minute

PAR : Protease Activated Receptor

PBS : Phosphate Buffered Saline

Rmp : Revolutions per minute

RNA : Ribonucleic Acid

RPMI : Roswell Park Memorial Institute medium

RT-PCR : Reverse Transcription Polymerase Chain

s : seconds

SDS : Sodium Dodecyl Sulfate

T : Thrombin

TF : Tissue Factor

TNF-α : Tumor Necrosis Factor Alpha

U : Unit

UI : International Units

VE-cad : Vascular-Endothelial Cadherin

VEGF : Vascular Endothelial Growth Factor

FIGURE INDEX

RESUMEN

Diversos estudios han demostrado una alta asociación entre hipercoagulabilidad sanguínea y la progresión del cáncer. La principal consecuencia de esta asociación es el desarrollo de cuadros de trombosis venosa, la cual es la segunda causa de muerte en pacientes oncológicos. Sin embargo, se desconocen ciertos mecanismos asociados al efecto de la vía de coagulación en diversos aspectos relacionados a la progresión del cáncer. Por lo tanto, analizamos el efecto del factor de coagulación Xa (FXa), una proteína central de la vía de coagulación, sobre el crecimiento tumoral y en la metástasis experimental de células de cáncer. El tratamiento intravenoso con FXa aumentó el crecimiento tumoral y la metástasis de células de melanoma murino (B16F10) al hígado, riñón y ganglios linfáticos. Tras la administración concomitante del anticoagulante anti-FXa Dalteparina, la metástasis pulmonar se redujo significativamente y no se observó metástasis en otros órganos. FXa no alteró directamente la proliferación, migración o invasión de células cancerosas *in vitro*. Por otro lado, FXa aumentó la formación de fibras de estrés, promoviendo así la disrupción de la VE-cadherina en la membrana y en consecuencia un aumento en la permeabilidad endotelial. Adicionalmente, células endoteliales tratadas con FXa mostraron un aumento en las moléculas de adhesión ICAM-1 y VCAM-1, lo cual promovió la adhesión de células B16F10. Un análisis realizado mediante un Microarray demostró que células endoteliales tratadas con FXa expresaron mayores niveles de transcritos inflamatorios en comparación al control, lo cual se relacionó con un incremento en la infiltración de células inmunes en los pulmones de ratones tratados con FXa. En conjunto, nuestros resultados sugieren que FXa incrementa la metástasis de células B16F10 a través de la activación de células endoteliales, lo cual apoya el concepto de que el sistema de coagulación no es simplemente un espectador en el proceso de metástasis del cáncer.

ABSTRACT

Hypercoagulable state has been intimately linked to cancer progression, however, the precise role of the coagulation cascade is poorly described. Herein, we examined the contribution of a hypercoagulative state through the administration of intravenous Coagulation Factor Xa (FXa), on the growth of solid tumors in mouse models of two human cancers and the experimental metastasis of the B16F10 mouse melanoma in a syngeneic model. The activated coagulation factor increased solid tumor volume and increased lung, liver, kidney and lymph node metastasis of tail-vein injected B16F10 cells. Concentrating on the metastasis model, upon co-administration of the anticoagulant Dalteparin, lung metastasis was significantly reduced, and no metastasis was observed in other organs. FXa did not directly alter proliferation, migration or invasion of cancer cells *in vitro*. Alternatively, FXa acted upon endothelial cells to promote cytoskeleton contraction, disrupt membrane VE-Cadherin pattern, to heighten endothelial-hyperpermeability, to increase the inflammatory adhesion molecules ICAM-1 and VCAM-1 and enhance B16F10 adhesion under flow conditions. Microarray analysis of endothelial cells treated with FXa demonstrated elevated expression of inflammatory transcripts. Accordingly, FXa treatment increased immune cell infiltration in mouse lungs, an effect reduced by Dalteparin. Taken together, our results suggest that FXa-increases B16F10 metastasis via endothelial cell activation and enhanced cancer cell-endothelium adhesion, which support the concept that the coagulation system is not merely a bystander in the process of cancer metastasis.

1. INTRODUCTION

1.1 Coagulation and cancer

The first observation linking exacerbated thrombus generation in cancer patients came from Dr. Armand Trousseau in 1865. Cancer presence has been related to coagulation cascade promotion and platelet activation, which can impinge tumor biology and generates a chronic hypercoagulable state in patients (Noble et al., 2010). As a consequence, venous thrombosis (VT) is the second leading cause of death among cancer patients worldwide (Elyamany et al., 2014; Falanga et al.,2013). The probability to suffer a thrombotic event is associated with the cancer type (e.g: brain, gastric and pancreatic cancer patients are more likely to develop VT) and the presence of risk factors, including chemotherapy regimens, high platelet count, and obesity favor such events (Muñoz Martín et al., 2018). Altogether, environmental factors and co-morbidities play a role in the development of a thrombotic event in cancer patients.

Several studies in the field identified a relationship between the cancer stage and the development of VT, in addition to the tumor origin. Interestingly, a high occurrence of venous thromboembolism in stage IV melanoma patients was found in a retrospective study (Sparsa et al., 2011), showing similar percentages of affected patients with lung and gastrointestinal cancers (both with high prevalence of VT). Moreover, in melanoma patients there is an association of high D-dimer levels (final product of the coagulation cascade activation) with an advance cancer stage and a positive correlation with poor prognosis and survival (Desch et al., 2016).

Altogether these findings suggest a strong contribution of coagulation cascade activation and thrombosis to cancer progression.

1.2 Coagulation cascade proteins in tumor cells and in their microenvironment

Tissue factor (TF) is a membrane protein, which, when in contact with blood, initiates the extrinsic pathway of the coagulation cascade by binding to Coagulation Factor VIIa (FVIIa) (Kasthuri et al., 2013; Henriquez et al.,2011). The complex TF-FVIIa promotes the formation of Coagulation Factor Xa (FXa) via proteolytic cleavage and the subsequent initiation of the common pathway of the coagulation cascade (Krupiczoic et al., 2008). TF is expressed in response to pro-inflammatory and pro-apoptotic factor exposure in endothelial cells and in the cell-microenvironment, like macrophages, neutrophils and fibroblasts. Additionally, Tissue Factor has been reported to be overexpressed in different tumor types (and in non-adherent cancer cells), suggesting a contribution to coagulation cascade activation in tumor biology. Moreover, chemotherapeutic drugs can stimulate the activation of the coagulation cascade by increasing TF levels or by decreasing Tissue Factor Protein Inhibitor-1 (TFPI-1), a protein that specifically binds TF acting as an inhibitor of the proteolytic activity of the TF-FVIIa complex (Haddad et al., 2006) Additionally, other mechanisms have been proposed associated to chemotherapy-procoagulant effect, including cellular stress and apoptosis of endothelial cells (Kirwan et al., 2015). Isolation of platelet and endothelial-derived microvesicles from melanoma patients showed a procoagulant potential compared to healthy subjects, suggesting an association of melanoma presence with thrombogenesis (Laresche et al., 2014).

1.3 Non-hematological functions of coagulation factors

Coagulation factor X (FX) plays a central role in the coagulation cascade. Synthesized in the liver, FX and can be proteolytically activated to form FXa. Activation may occur via the extrinsic or the intrinsic coagulation pathways. Once activated FXa unleashes a

proteolytic cascade that converts prothrombin into Thrombin, leading to the formation of fibrin networks, platelet activation eventually generating a blood clot. Besides their role in the coagulation cascade, both FXa and Thrombin can also act as activators of Protease Activated Receptors (PARs) triggering different responses in several cell types such as: fibroblasts, platelets, endothelial and cancer cells (Zigler et al.,2011; Han et al, 2011). Accordingly, FXa via PAR-1 activation can inhibit breast, colon and lung cancer cell line migration (Borensztain et al., 2011). In endothelial cells, FXa and Thrombin increase the expression of pro-inflammatory molecules, such as interleukin 6 and 8 (IL-6 and IL-8) (Zigler et al., 2011; Senden et al., 1998). Furthermore, the anti-inflammatory effect of human-FVIIa has been demonstrated through intravenous administration in mice (Kondreddy et al., 2018), suggesting an independent role of coagulation factors over inflammatory responses. The relation between the coagulation pathway and inflammation has been addressed extensively, in which Thrombin (independent of FXa) appears to be the key molecule in this association (Ebrahimi et al., 2017).

1.4 Hematogenous metastasis and endothelial activation

Hematogenous metastasis is a highly ordered, stepwise process that starts when cancer cells acquire an invasive phenotype, detach from the primary tumor and enter the bloodstream, in a process termed hematogenous intravasation (Nguyen et al., 2009). The cancer cells subsequently can migrate to distant organs and establish metastatic foci after extravasation from the bloodstream. Extravasation first requires the attachment and firm adhesion of the cancer cell to the endothelium. This process is mediated principally by integrins and selectins expressed both in the cancer and on the endothelial cell (Läubli et al., 2010; Bendas et al., 2012; Ferjancic et al., 2013). Endothelial selectins, such as: P-selectin, E-selectin, and the intercellular adhesion

molecules ICAM-1, VCAM-1 and their ligands, have been related to immune cell and cancer cell adhesion to the vasculature (Kolaczkowska et al., 2013). All these adhesion molecules are expressed in response to a pro-inflammatory stimulus (such as TNF-α, LPS or IL-1β) from a damaged tissue, triggering the extravasation and infiltration of monocytes and neutrophils into the target tissue. The ligands of these adhesion molecules are expressed mainly in immune system cells; however, their expression has also been observed in cancer cells. Schlesinger et al (2014) demonstrated the expression of VLA-4 in B16F10 murine melanoma cells, also elucidating their contribution to the metastasis. After firm adhesion, cancer cells must transverse the highly selective endothelial barrier. The permeability of the endothelial barrier is principally maintained by adherence junctions and occludines, of which the most studied protein is the Vascular Endothelial cadherin (VE-cadherin) (Vestweber et al., 2008). Under inflammatory conditions, the VE-cadherin complex disassembles (Lampugnani and Dejana, 2007), promoting vascular hyperpermeability and allowing the extravasation of immune cells into the target tissue. Cancer cells can exploit this physiological process to facilitate metastasis (Reymond et al., 2013). Interestingly, *in vitro* observations showed that thrombin promotes endothelial hyperpermeability through the activation of the small GTPase RhoA (van Nieuw et al., 2000).

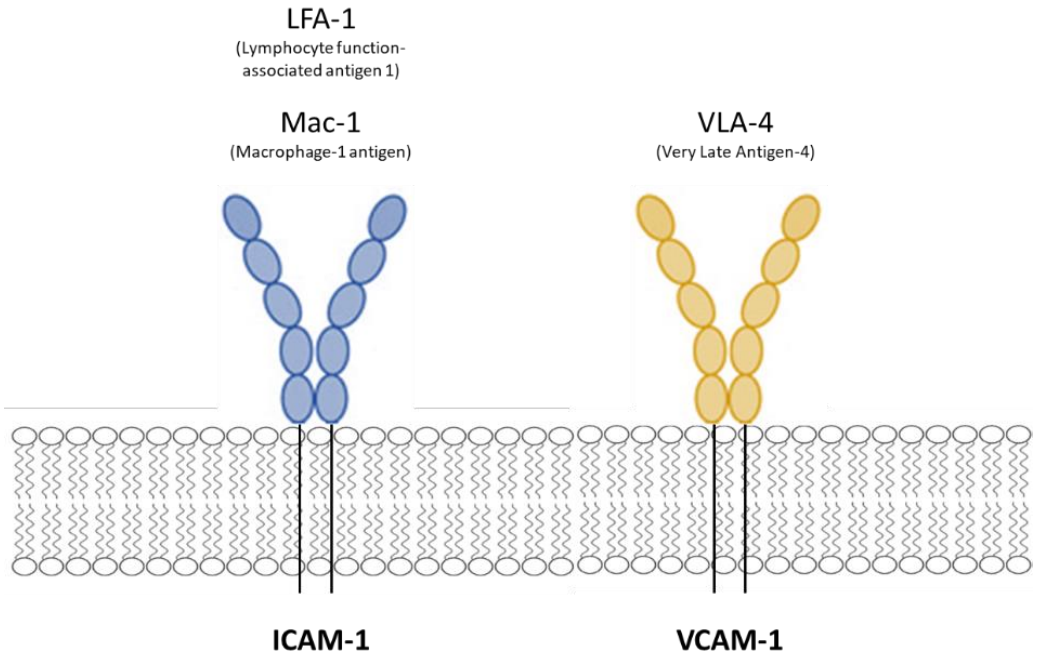

Figure 1. Endothelial ICAM-1 / VCAM-1 and their ligands: LFA-1, Mac-1 and VLA-4. Adhesion molecules are expressed on endothelial cells in response to pro-inflammatory stimuli (eg. TNF-α, IL-1 or LPS) or upon activation of the coagulation cascade (Thrombin). The ligands of these molecules are principally expressed in monocytes or neutrophils and mainly serve as an anchor of adhesion to the endothelium and thus facilitate its extravasation. A cumulative number of studies suggest that the VCAM-1/ICAM-1 ligands could be expressed in cancer cells and participate in the metastasis process.

1.5 Anticoagulants regime in cancer patients

Previous reports suggest that Direct Oral Anticoagulants (DOACs, specific protease inhibitors of the coagulation cascade) increase survival rates among cancer patients (Gerotziafas et al., 2008). In contrast, the *FRAGMATIC* trial found that the adjuvant Dalteparin (a low molecular weight heparin anticoagulant) had no effect upon survival rates in advanced lung cancer patients (Griffiths et al., 2009). Despite the negative results with Dalteparin, a similar trial found that its

use in combination with chemotherapy increased survival rates among lung small-cell carcinoma patients (compared to patients that only received chemotherapy) (Altinbas et al, 2004). Significantly, a twelve-month treatment with Dalteparin in a multiple-cancer clinical trial showed an increase in the overall survival in a subgroup of patients with better prognosis, suggesting a potential role of this drug over metastasis and tumor biology (Kakkar et al., 2004). The use of anticoagulants in cancer patients is still controversial and their use as an adjuvant treatment is under debate, in part due to the potential side effects, such as thrombocytopenia and spontaneous hemorrhage. However, their safeness has been demonstrated over numerous clinical trials on cancer patients, therefore the possibility to use anticoagulants as a prophylactic treatment is still under evaluation. The current clinical and *in vivo/viro* studies suggests that the coagulation system may not be merely a bystander in the process of cancer metastasis, indeed is an escential physiological axis. In that line, we propose that the hypercoagulable state observed in many cancer patients, not only increases the risk of thrombosis, but may alter endothelial barrier properties and thus promoting cancer cell metastasis.

Taken together, clinical and *in vivo/vitro* studies suggest a role of the coagulation system in inflammation and metastasis; however, the mechanisms are still elusive. Thus, we studied the contribution of the central protein of the coagulation cascade, FXa, to metastasis and the role of endothelial cells in this process.

2. HYPOTHESIS

The Coagulation Factor Xa (FXa) promotes melanoma metastasis by increasing endothelial permeability and enhancing tumor-endothelial cell adhesion.

3. OBJECTIVES

3.1 General Objective

Analyze the contribution of FXa to the metastasis of B16F10 cells and its effect on the activation of endothelial cells.

3.2 Specific Objectives

1- To determine the contribution of FXa to the metastasis of B16F10 cells in C57BL/6 mice.

1.1 Analyze lung and other organ metastasis of B16F10 cells injected into C57BL/6 mice intravenously treated with FXa using short-term and chronic regimens.

1.2. Analyze lung and other organ metastasis of B16F10 cells injected into C57BL/6 mice intravenously treated with FXa in combination with the anticoagulant Dalteparin.

1.3 Evaluate the immune infiltration (over lungs) in response to FXa and Dalteparin treated mice.

2- Determine the effect of FXa on B16F10 *in vitro.*

2.1. Evaluate the effect of FXa on cell viability and proliferation, using WST-1 and flow cytometry.

2.2. Determine changes in the migration and invasion of B16F10 cells treated with FXa, using wound closure assays and Transwell systems, respectively.

2.3. Analyze changes in the expression of homing-related molecules in B16F10 with FXa by flow cytometry.

3. Analyze the endothelial activation in response to FXa exposure.

3.1. Determine the effect of FXa treatment over already formed tubular like structures formed by endothelial cells on Matrigel.

3.2. Evaluate the formation of stress fibers and determine the cell area in endothelial cells treated with FXa by immunofluorescence.

3.3. Evaluate changes in the VE-cadherin, RhoA and pFAK pattern in endothelial cells treated with FXa.

3.4. Determine the effect of FXa treatment over different genes related to endothelial cell biology using microarrays.

3.5 Analyze the endothelial barrier permeability to macromolecules in response to FXa *in vitro and in vivo.*

4. Determine the effect of FXa on the adhesion of B16F10 and endothelial cells co.-cultures.

4.1. Determine the changes in VE-cadherin, ICAM-1 and VCAM-1 total protein levels in endothelial cells treated with FXa.

4.2. Evaluate changes in the adhesion of B16F10 to endothelial cells pre-treated with FXa under static/flow conditions.

4.3. Evaluate the mRNA levels of ICAM-1/VCAM-1 ligands on primary tumor and metastasis samples of melanoma patients using the TCGA-TIMER data base.

4. MATERIALS AND METHODS

4.1. Reagents and cell culture

FX(a) were purchased from Haematologic Technologies (CXA-0060). Antibodies were purchased from the following companies: VCAM-1 and ICAM-1 (Santa Cruz), pFAK (Abcam), Vimentin (Abcam), Actin (Sigma), VE-, E- and N-cadherin (Cell Signaling). Matrigel Growth Factor Reduced (Corning 354230) and Phalloidin-Rhodamine (ThermoScientific) were purchased from local distributors. Dalteparin 2500UI (Pfizer) was purchased directly from the pharmacy and diluted in sterile saline solution.

The endothelial cell line EAhy926 (CRL-2922) and the melanoma cell line B16F10 (CRL-6475) cells were purchased from the ATCC. B16F10-eGFP cells were purchased from Imanis Life Science (CL053, Rochester, USA). The human melanoma cell line Mel-1 was kindly donated by Dr Lopez and Dr. Salazar (University of Chile). Ishikawa cells were donated by Dr. John While (Hammersmith Hospital, London UK) and HPMEC-1 were kindly provided by Dr. Claudia Sáez (Catholic University of Chile). Primary cultures of Human Umbilical Vein Endothelial Cells (HUVECs) were isolated from fresh umbilical cords and obtained as previously described (Torres-Estay et al., 2016). All procedures were approved by the Ethics committee of Pontifical Catholic University. All cells were cultured at 37°C, 5% CO_2 in DMEM-F12 medium (Dulbecco's Modified Eagle Medium), IMDM (Iscove's modified Dulbecco's medium), Growth Medium MV supplemented with endothelial growth factors or SFM (Serum free media supplemented with Endothelial cell growth factors) and 10% FBS (S1810, Biowest, France).

4.2. Flow cytometry

Cell cycle and chemokine receptor analysis was done as previous described (Oyarce et al., 2017). Briefly, B16F10 and Mel-1 cells were treated with FXa or vehicle (water) for 24h, then fixed with ice-cold 70% ethanol and incubated with propidium iodide (0.5 mg/ml). Stained nuclei cells were analyzed by flow cytometry (FACSsan) and the fraction (sub-G0/G1, G0/G1, G2/M and S phase) determined as a percentage of the total cell population using the Cell-Quest program (Beckton-Dickinson).

For the analysis of chemokine receptor expression in B16F10, cells were treated with FXa for 24 h and harvested after 3 min incubation with 0.25% trypsin-EDTA solution. Then cells were washed once with PBS/FBS 2%. Samples were stained with antibodies for 30 min (αCD62L-PE, αCXCR3-Percp, αCCR8-APC, αCCR7-Pacific Blue and Zombie-aqua for cell viability). Cells were washed two times with PBS / FBS 2% and then analyzed by flow cytometry.

4.3. Regression assay

Eahy926 and HUVECs (30.000 cells) were seeded onto 48 well pre-coated with non-diluted Matrigel. To promote tubular like structure formation, VEGF 10ng/mL (in serum free media) was added. After 8 h, the maximum formation of capillary like structures was observed and FX(a) was added. Several images from same fields were taken at 0, 2 and 4 h after the addition of FXa and the disassembly of the already-formed tubular like structures was determine using the Angiogenesis Analyzer plugin from ImageJ. Master segments were quantified and expressed as the percentage of linked networks, assuming 0h as a 100%.

4.4. *In vitro/ in vivo* permeability assay

EA.hy926 cells were grown to a 100% confluent monolayer in 3 µm pore Transwell inserts (PITP01250, Merck-Millipore) pre-coated with 1% gelatin. Then, permeability was analyzed using Evans Blue as described by Patterson et al (1992) with minor modifications. Briefly, the upper compartment was filled with 400µL of serum-free media in the presence of FXa. After 30 min of incubation, upper media was replaced with Evans Blue (0.67mg/mL) and 4% BSA dissolved in serum free culture media and 1.5mL of fresh culture media was added into the lower chamber. 100µL aliquots were collected from the lower chamber every 15 min and optical density was analyzed at 650nm in a 1:3 dilution.

Animal protocols were approved by the Institutional Bioethics and Biosecurity Committee at the Universidad Austral de Chile and conducted according to NIH Guidelines. Microvascular permeability to macromolecules was measured by intravital microscopy in the mouse cremaster muscle according to published methods (Zamorano et al., 2012; Durán et al., 2000). Briefly, C57BL/6 male mice (30-50g) were anesthetized with Ketamine 80 mg/kg Xilazine, 8 mg /kg I.P; and the left cremaster muscle was prepared for intravital microscopy, by exposing the tissue and placing it in an ad hoc observation chamber, under constant perfusion with bicarbonate buffer as described. FITC-Dextran 70 kDa (100 mg/kg i.v.) was injected as a fluorescent macromolecular tracer. Plasma to tissue transport was evaluated *in situ* by integrated optical intensity (IOI). FXa was added topically in the cremaster for 15 min. At the end of the experiment, the animal was sacrificed by an anesthetic overdose (~300 mg/Kg iv), followed by euthanasia.

4.5. Immunofluorescence

HUVECs cells were grown to high/low confluence state on glass coverslips. Then treated with FXa (20 and 130nM) in serum free media and fixed with 4% PFA at room temperature. Cells were then washed with 1X PBS and incubated with PBS-Triton 0.1% for 5 min and blocked with 2% BSA-PBS for 30 min at room temperature. Primary antibody was incubated overnight in a humid chamber at 4 °C and the secondary antibodies (Anti-rabbit Alexa Fluor 488 and 555) and Phalloidin-Rhodamine were incubated for 1h at room temperature. Cell nuclei were stained by DAPI and coverslips were mounted using Fluoromount (1798425, Fisher Scientific, USA). Images were obtained from independent fields for each coverslip in a Nikon C2s1 microscope and processed/analyzed in ImageJ (NIH). To evaluate the localization and recruitment of the active form of RhoA in response to FXa, HUVECs were treated in serum free media for 5 min, fixed with Trevors fixation buffer and maintained in Universal buffer. After that, fixed cells were subjected to Far-IFI to analyze the active form of RhoA (Bustos et al., 2012). Cells were permeabilized with Triton 0.1% and blocked using BSA 2% for 30 min. Cells were incubated with anti RhoA-GST cassette (dilution 1:25) for 2h at room temperature in humid chamber. Anti-GST (1:100), anti-mouse Alexa Fluor 488 (1:300) and Phalloidin-Rhodamine (1:500) were incubated for 1h at room temperature in a humid chamber. Cells were mounted with Mowiol embedding medium and visualized using epifluorescence microscopy (Nikon C2s1).

4.6. Underflow and static adhesion assay

HUVECs were plated and grown to 100% confluence on a 48-well plate. Cells were treated with FXa for 4h. 10,000 B16F10-eGFP cells were added on top of the endothelial cell monolayer and incubated for 30 min. The well was washed with warm 1X PBS to remove unattached B16F10-

eGFP cells, before fixing for 20 min with PFA 4%. Visualization was by epifluorescence microscopy Nikon C2s1 and quantification was with the ImageJ software.

HUVEC were seeded in a gelatin-coated microchannel slide (ibiTreat µSlide Luer $I^{0.4}$; Ibidi; Ref.80176) and cultured in Endothelial Cell Basal Medium with full supplements (PromoCell, EBM-MV2) until reaching confluency at 37°C and 5% CO_2/95% air in a humidified chamber. B16F10 cells ($1.7x10^6$ cells/mL) were pumped into the microchannel slide under 50ul/min flow speed using a syringe pump (NE-1200X; New Era Pump System) enabling B16F10 cells to interact with the monolayer of control or FXa pre-treated HUVEC. Adhesion of B16F10 cells to the endothelial monolayer was monitored using a Leica SP8 microscope equipped with a motorized xyz stage and with a temperature-controlled CO_2-incubation system for live cell time-lapse imaging.

Differential interference contrast (DIC) images of 3 distinct areas along the microchannel were taken using 10x objective every 10s during a total of 25 min. The number of B16F10 cells adhering to the HUVEC monolayer was quantified by ImageJ software.

4.7. Cell migration and invasion

For the Scratch assay (wound healing assay), 6-well plates with 100% confluent B16F10 cells were used. A scratch was made with a yellow pipette tip. The plate was treated with FXa or its vehicle in serum free medium. The plate was photographed at different time points until total wound closure was observed. The area of wound closure was quantified with ImageJ.

To analyze cell invasion, Transwell inserts containing membranes with 8 µm pore size (Millicel) were coated with growth factor reduced Matrigel as described (Erices et al., 2017). 50.000 B16F10 cells were seeded over the matrigel (1:5 dilution in serum free media) and 800 µL of

10% of serum medium was added to the lower chamber as a chemoattractant. FXa was added to the upper chamber together with cells, at a final concentration of 130nM and cells were allowed to invade for 8h. To assess the number of invaded cells, transwells were fixed with warm 4% PFA for 20 min at room temperature and stained with crystal violet for 10 min. The membranes were removed and mounted on cover slides with warm 10% gelatin (Merck). At least 10 images at 10X magnification were taken per treatment and the number of cells on the underside of the filter were counted.

4.8. WST-1 proliferation assay

B16F10 were seeded into 96-well dishes and treated with FXa for 24h. After that, cells where incubated with the colorimetric reagent WST-1 for 15 min approximately. The absorbance (at 490nm vs 620nm) was analyzed and graphed as the percentage of cell viability.

4.9. Western Blot

HUVECs were incubated with FXa in serum free media before protein extraction using lysis buffer supplemented with protease inhibitors. Proteins were quantified by the Bradford method and separated by SDS-PAGE (in 12% gels) for 1.5h at 100 volts. Samples were transferred to nitrocellulose membranes for 2h at 300mA (Wet/Tank Blotting Systems, Bio-Rad). The membranes were blocked with TBS-Tween 5% Milk and the primary antibodies (1:500 dilution) were incubated overnight at 4 °C. The secondary antibody (anti rabbit/mouse-HRP 1:3000 dilution) was incubated for 1h at room temperature and labeled proteins were identified using the myECL system (Pierce Biotechnology).

4.10. Metastasis and tumor growth *in vivo* experiments

All protocols and animal management were performed in accordance with guidelines established by the Bioethics Committee of the respective institutions. Animal studies using Ishikawa endometrial cells in NIH nu/nu mice (purchased from the Universidad Nacional de La Plata, Argentina) were performed at the animal facility of the Pontificia Universidad Católica de Chile. Mel-1 melanoma studies were performed in NOD/SCID mice purchased from the animal facility at the University of Chile. B16F10 melanoma cells were injected into C56BL/6 mice at the animal facility of Andes Biotechnologies within the Science and Life Foundation, Santiago, Chile. Briefly, to analyze metastasis, 7-9 week old male and female C56BL/6 mice were injected via the tail vein with 200,000 B16F10 (in 400µL of sterile saline solution). Analysis of a hypercoagulative state through the administration of intravenous coagulation factors has been reported previously (28). As addition was via intravenous injection, FXa was added at a circulatory concentration of 130nM into the tail vein twice a week for up to 21 days. Dalteparin (final concentration 200UI/kg, diluted in 150 µL of saline solution) was injected subcutaneously 30 min before FXa administration. For the analysis of solid tumors of human cancer cell lines, Ishikawa cells ($5x10^6$ cells) or Mel-1 cells ($2x10^6$ cells) were injected subcutaneously into the flank of the immunocompromised female NIH nu/nu mice and NOD/SCID mice respectively. FXa, FX or vehicle (PBS) was added intravenously every 2 days for 21 days. Animals were sacrificed and autopsied before they reached the maximum tumor size established by the bioethics protocol.

4.11. Microarray analysis

Endothelial cells (EA.hy926) were treated with FXa 130nM for 4h in serum free media. The RNA extraction was performed using an RNA isolation kit. A total of 6 samples were assayed on Affymetrix whole transcriptome expression (Affymetrix HuGene-2_0-st-v1) in which 53.617 transcripts were analyzed. The data was processed at the Microarray Facility at The Centre for Applied Genomic, Sick Kids hospital, Toronto. All steps were performed with the statistical analysis program R version 3.2.0 (https://cran.rproject.org/), using the Bioconductor package oligo version 1.32.0. Once the samples were filtered, the Differential Expression Analysis was carried out, contrasting the two study groups, using Linear Models for Microarray Analysis, Limma. A Fold Change, FC = 1 and a p value <0.05 were established, thus obtaining 127 overexpressed genes and 37 genes were down-regulated in the cells. The algorithm of Benjamini and Hochberg was used to adjust the p-value and eliminate the false positives from the analysis. The whole final data analysis was performed in the CORE biodata facility of Advance Center for Chronic Diseases (ACCDiS) center.

4.12. Statistical analysis

For the comparison of the data obtained between treatments, an ANOVA or t-test statistical analysis was performed followed by a Bonferroni post-test, considering a value of P <0.05 as statistically significant. For the *in vivo* experiments a minimum of 3 animals were used per group.

5. RESULTS

5.1 FXa increased tumor growth and metastasis *in vivo*

To determine the effect of FXa on tumor growth, we examined the treatment of this activated coagulation factor on the growth of solid tumors in mice. To this end, we subcutaneously introduced the Ishikawa human endometrial cancer cells into the flank of immunosuppressed NIH nu/nu mice and the human melanoma cell line Mel-1 into the flank of NOD/SCID mice. As shown in figure 1, intravenous FXa increased the solid tumor mass of both the endometrial cancer model and the human melanoma cell tumor (Fig 2 A and B). No metastases were observed upon autopsy in either model. Recombinant zymogen FX did not influence tumor growth (Fig 2A).

To assess the contribution of the FXa in the metastasis, B16F10 cells were injected into the tail vein of C57BL/6 and mice were treated with FXa or vehicle intravenously three times a week until completing the 21 days of experimentation. Representative images of the lung metastasis (Fig 2C), reveal an increased tumor burden in the FXa group. Significantly, FXa increases the metastasis to other organs (spleen and lymph node), which is uncommon in this melanoma metastasis model. Mice that were treated with FXa showed a similar behavior and phenotype as the control mice and only in the last day of experimentation showed features related to advanced cancer.

Our next aim was to elucidate a possible mechanism of action by which FXa was increasing metastasis and tumor burden. Therefore, our first approximation was evaluated the response of cancer cells to FXa exposure *in vitro*.

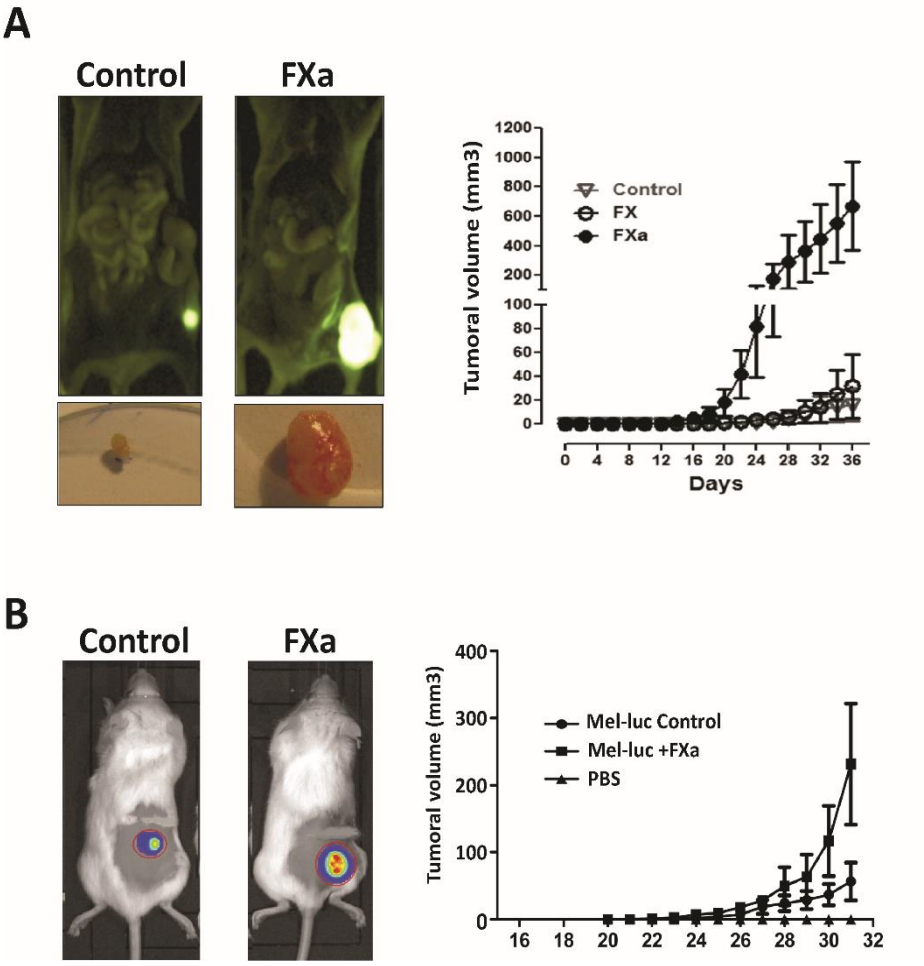
A
Control
FXa
Tumoral volume (mm3)
1200
1000
800
600
400
200
100
80
60
40
20
0
Control
FX
FXa
0 4 8 12 16 20 24 28 32 36
Days
B
Control
FXa
Tumoral volume (mm3)
400
300
200
100
0
Mel-luc Control
Mel-luc +FXa
PBS
16 18 20 22 24 26 28 30 32
C
Lung
Spleen
Lymph node
Control
FXa
CM 1

Figure 2. FXa injection increases tumor size in human endometrial cancer and melanoma models and promotes metastasis of B16F10 melanoma cells. (A) Human endometrial cancer (Ishikawa-ZsGreen) and (B) human melanoma cells (Mel-1-Luciferase) were injected subcutaneously in the flank of NIHnu/nu and NOD/SCID immunocompromised mice, respectively. FXa (at 130nM final concentration) was administrated intravenously every two days throughout the experiment. Tumor volume was determined using calipers in the endometrial cancer model and by IVIS chemiluminescence and calipers in the melanoma model. The equation TV (mm^3) = (long x $width^2$)/2 was used and results obtained in both models are shown. n=4 $p<0.05$ ANOVA. (C) B16F10 cells injected into the tail vein of C57BL6 mice. FXa or vehicle was administered intravenously every 48 h for 3 weeks n=4.

5.2 The anticoagulant Dalteparin inhibits the pro-metastatic effect of FXa in mice.

B16F10 cells were injected into the tail vein of C57BL/6. Mice were treated with FXa or vehicle intravenously three times a week until completing 21 days of experimentation (chronic regime). Representative images of the lung metastasis(Fig 3A), revealed an increased tumor burden in the FXa group. Additionally, other organs were affected only in the FXa group, suggesting that FXa is increasing the metastasis and changing the homing of B16F10 cells.

An anticoagulant treatment (with the low molecular weight heparin Dalteparin, 200UI/kg) was administered sub-cutaneously to mice alone and in combination with FXa intravenous injections. Dalteparin treatment inhibited the pro-metastatic effect of FXa in this mouse model (Fig 3A & B). The effect of the zymogen FX injection showed no statistical differences compared to the control group (data not shown). Notably, liver, kidney, spleen and lymph nodes metastasis were observed only in mice treated with FXa (Fig 3C) and Dalteparin treatment prevented the appearance of metastasis outside the lung. The anticoagulation regime was well tolerated during the experiment.

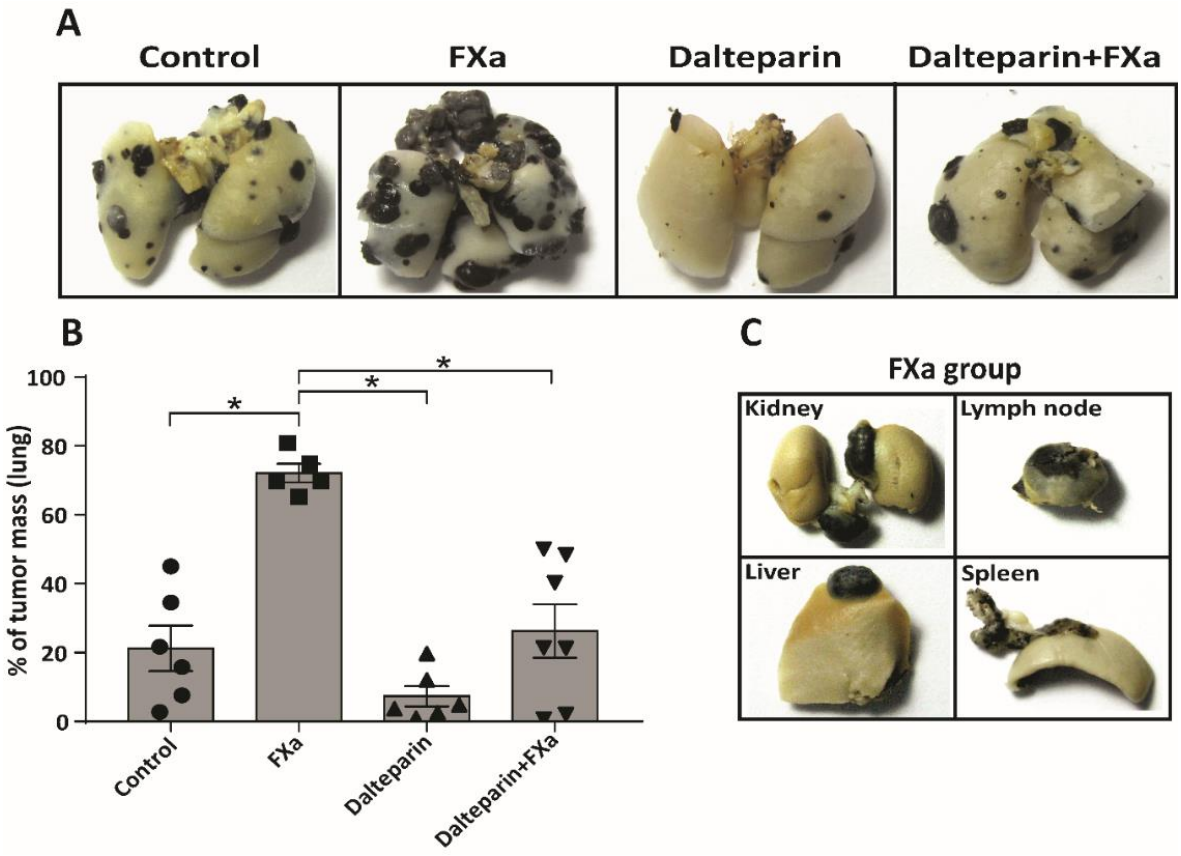

Figure 3. FXa promotes melanoma metastasis, an effect reduced by Dalteparin. (A) 200.000 B16F10 cells were injected into the tail vein of C57BL/6 mice and FXa (or vehicle, control) was administrated intravenously twice a week until euthanasia at 21 days. The anticoagulant Dalteparin was injected sub-cutaneously 30 min before FXa administration. Representative images from metastasis-affected lungs are shown. (B) Quantification of lung tumor burden was assessed through the weighing of total lung mass and the dissected tumor mass. $p<0.05$ ANOVA, post-test Bonferroni. (C) Representative images of organ metastasis found exclusively in mice from the FXa group

5.3 FXa did not modify cancer cell proliferation, migration, invasion nor homing-related proteins *in vitro*.

Next, we sought to determine the mechanism by which FXa increases tumor growth and metastasis. First, we hypothesized that FXa has an effect upon cancer cells.

As a first approximation, Ishikawa and Mel-1 were treated with FXa (130 nM) for 24h to analyze cell cycle using the cellular DNA content as a parameter (Fig 4A & B). There were not statistical differences between sub G1, G0-G1, S-G2-M phases. This result suggests that cancer cells are not proliferating or entering into apoptosis/necrosis (peak in the sub G0/G1 phase) in response to FXa. Tumor cells that were subjected to FXa treatment did not exhibit changes in the Endothelial to Mesenchymal Transition (EMT) markers E-cadherin, N-cadherin and Vimentin (Figure 4D). Consequently, cell migration was not affected in cancer cells exposed to FXa (Fig 4C). The migration of the cancer cells was evaluated using the Transwell system, in which 10% FBS was seeded in the lower chamber as a chemoattractant and FXa was added to cells in the upper compartment as a treatment.

Next, the effect of FXa-treatment was evaluated in the murine melanoma cell line B16F10 *in vitro*. FXa addition (130nM) did not alter B16F10 cell migration (Fig 5A & B). Moreover, FXa treatment did not alter cell death (appearance of a sub G0/G1 peak by flow cytometry) or bring about significant changes in the cell cycle (Fig 5C). The lack of changes in proliferation was further confirmed using the colorimetric reagent WST-1, in which an increase in the absorbance is associated to a higher cell number (Fig 5D). Flow cytometry analysis confirmed that FXa did not change the levels of the cytokine receptors: CCR7, CCR8, CXCR3 and CD62L (Fig 5E). These receptors have been related to differential homing of cancer cells to distant organs, similarly to the figure 1C. Furthermore, invasion capabilities (evaluated using Transwells

system with Matrigel coating) were not affected in response to FXa (Fig 5F). Additionally, we tested whether FXa could stimulate pro-angiogenic factors when in contact with cancer cells; however the conditioned medium from cancer cells treated with FXa did not alter capillary-like formation by the endothelial cells.

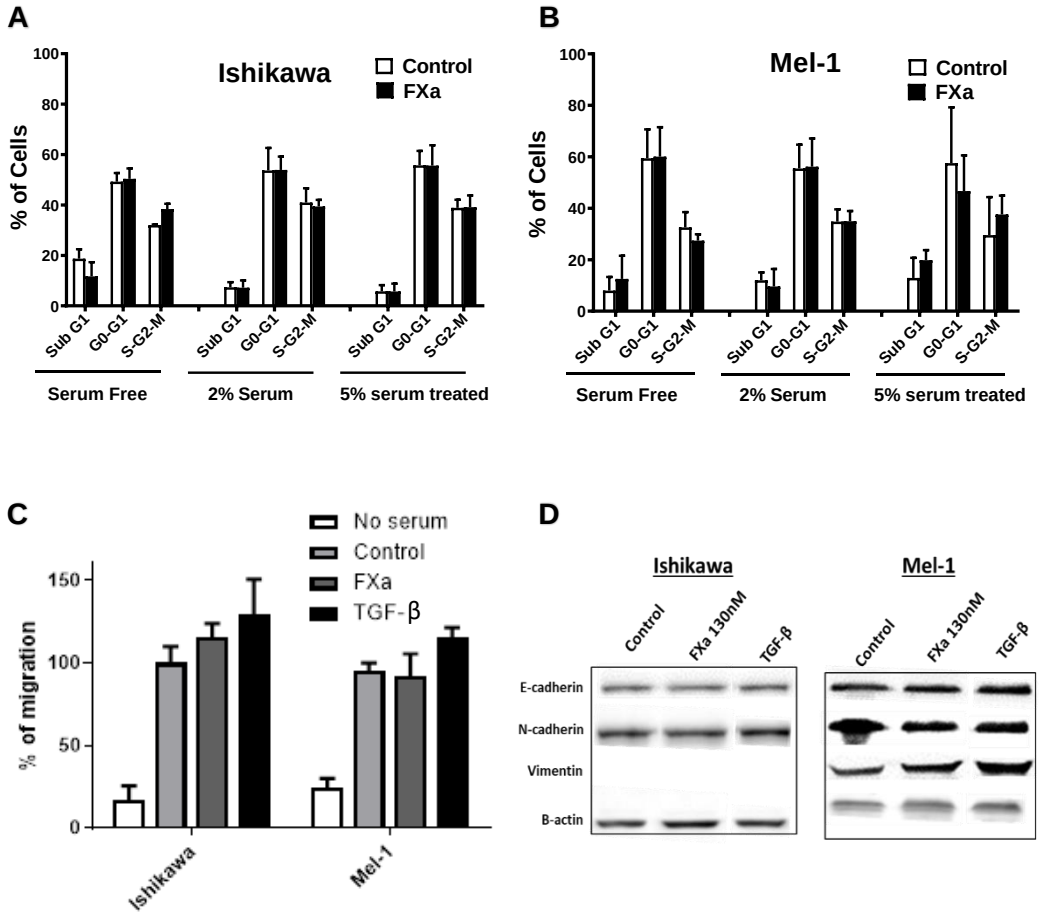

Figure 4. FXa did not change cell cycle, migration or Epithelial Mesenchymal Transition (EMT) markers in Ishikawa and Mel-1 cells. Ishikawa (A) and Mel-1 (B) were treated with FXa for 24h and the subjected to cell cycle analysis using flow cytometry. (C) The migration of both cell lines was analyzed using transwell systems, promoting migration with 10% FBS in the lower chamber. Cells were co-treated with FXa or TGF-B and after 8h were fixed and stained with Violet Crystal. (D) Ishikawa and Mel-1 were treated with FXa or TGF- B (inductor of EMT) for 24h. EMT markers were visualized using Western Blotting in three different experiments. Representative images are shown. P>0.05, n=3.

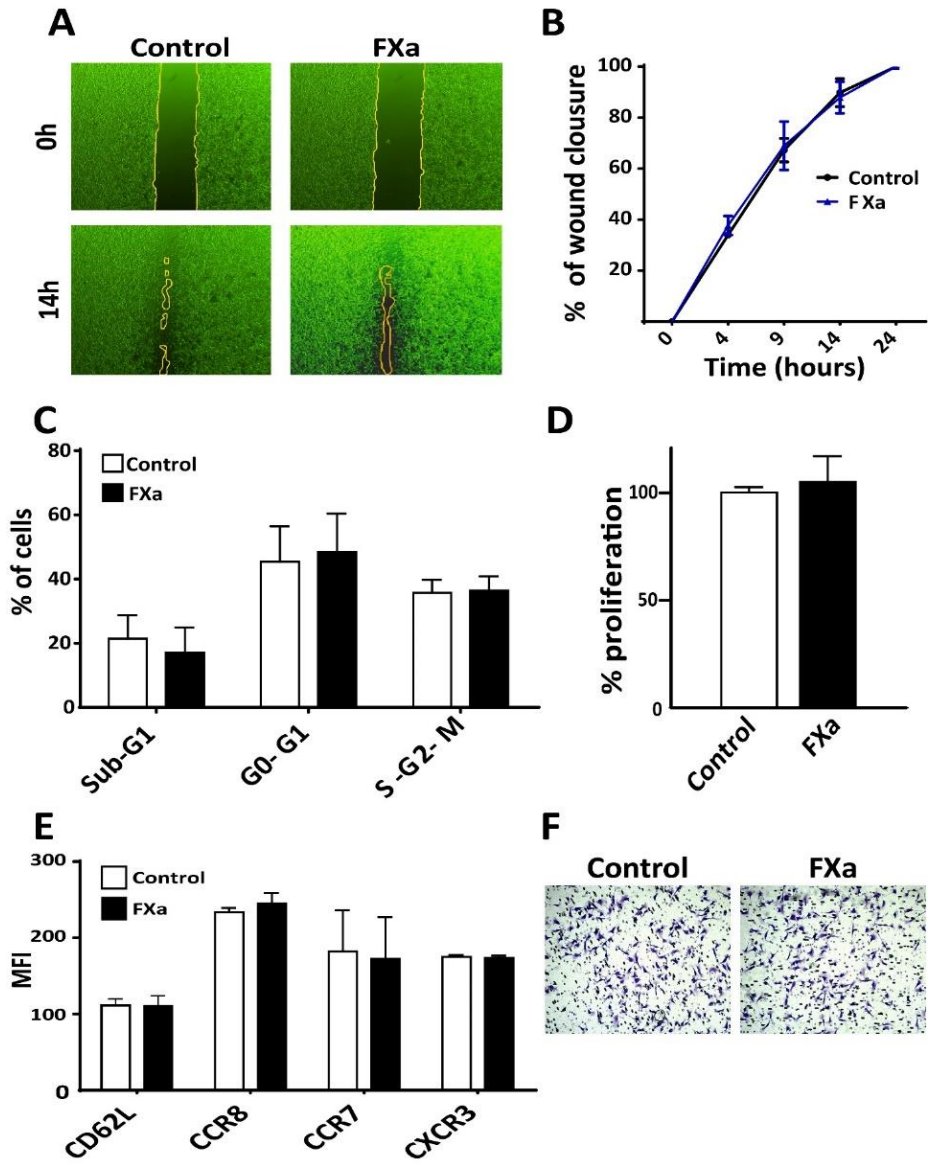

Figure 5. FXa does not alter cancer cell biology *in vitro*. (A) A scratch was generated upon a confluent B16F10 cell monolayer. After that, FXa or vehicle were added and (B) wound closure was evaluated through the time, n=3. (C) Cells were treated with FXa, fixed and stained with propidium iodide. Cell cycle was analyzed with flow cytometry. (D) Semi-confluent B16F10 were treated with FXa for 24h and proliferation was evaluated using WST-1, n=3. (E) The adhesion molecule CD62L and the chemokines receptors CCR8, CCR7 and CXCR3 levels in cancer cells were analyzed by flow cytometry in response to FXa treatment, n=3. (F) B16F10 were treated for 24h with FXa and placed to invade for 8h. Cells were fixed and stained with violet crystal**.** P>0.05

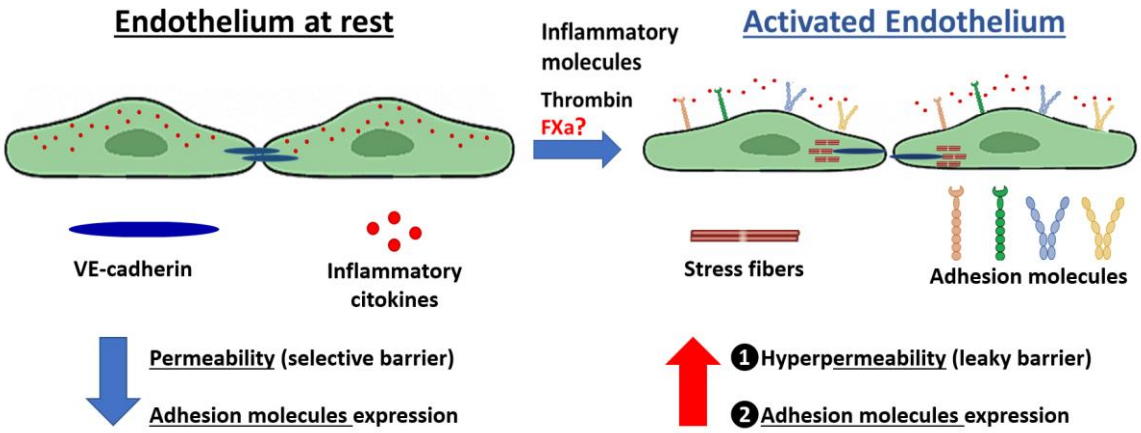

Figure 6. Endothelial activation: A link between coagulation and the inflammatory pathway. Pro-inflammatory molecules or Thrombin are released from an injury tissue or from an acute infection and trigger endothelial cell activation. Distinct chemokines (such as: IL-8, IL-6 and MCP-1) are released, and adhesion molecules (such as: VCAM-, ICAM-1 and E-selectin) are exposed to the bloodstream. Additionally, endothelial-hyperpermability occurs through stress fiber formation and the uncoupling of tight juctions (such as VE-cadherin). Under physiological conditions, this process promotes monocyte/neutrophil attachment, firm adhesion and extravasation to the inflammated tissue. The importance of FXa in endothelial activation and its relevance to cancer cell metastasis are poorly understood.

5.4 FXa disrupts tubular like structure formation in Matrigel

An increasing number of publications are suggesting a contribution of tumor microenvironment to cancer progression and metastasis. The hemostatic role of coagulant proteins and their up-regulation in cancer has been proposed as a main cause of Thrombosis in patients; however, the non-hemostatic effect on the pathogenesis and evolution of the disease is still unknown. The non-hemostatic function of coagulation proteins has been principally related to endothelial cells. Therefore, we proposed that this component of the tumor microenvironment represents a main actor in the pro-metastatic effect of FXa (Fig 6). Of note, Thrombin was employed in our experiments as a positive control for endothelial activation.

As shown in figure 6, there is a well-described link between the coagulation system and the inflammatory pathway, in which Thrombin represents the most studied protein. Here, we postulate that FXa independently of Thrombin is promoting endothelial cell activation and thus increasing the metastasis of tumor cells. The main aim of the following experiments was to determine the effect on the metastasis of the B16F10 melanoma cells, principally because metastasis is the main cause of death in cancer patients. Therefore , it was interesting to us to study the importance of the coagulation cascade pathway in this pathological process.

As a first approximation, changes in endothelial cell phenotype were analyzed in response to FXa. First, we used an angiogenesis assay culturing HUVECs in 3D matrigel wells. Under these conditions, endothelial cells form tubular-like structures, in which cells connect to each other and form polygonal elongations (Fig. 7). Our data showed a significant reduction in the percentage of tubular linked network after a 2h incubation with FXa (please refer to a time-lapse video of FXa-treated endothelial cells, http://www.labowen.cl/cgi-bin/Website/Pages/Internal.html.pl?PagId=51&). While cells were still attached to the Matrigel

and alive, neither elongation or migration was observed. Furthermore, this result was maintained 24h post-treatment (not shown). The aforementioned results strongly suggest that FXa is increasing endothelial cell contraction.

This effect is specific for the protease activity of FXa since the treatment with the zymogen (FX) did not lead to differences compared to the control (Fig 8). Given these findings, we next assessed the response of endothelial cells at cellular level.

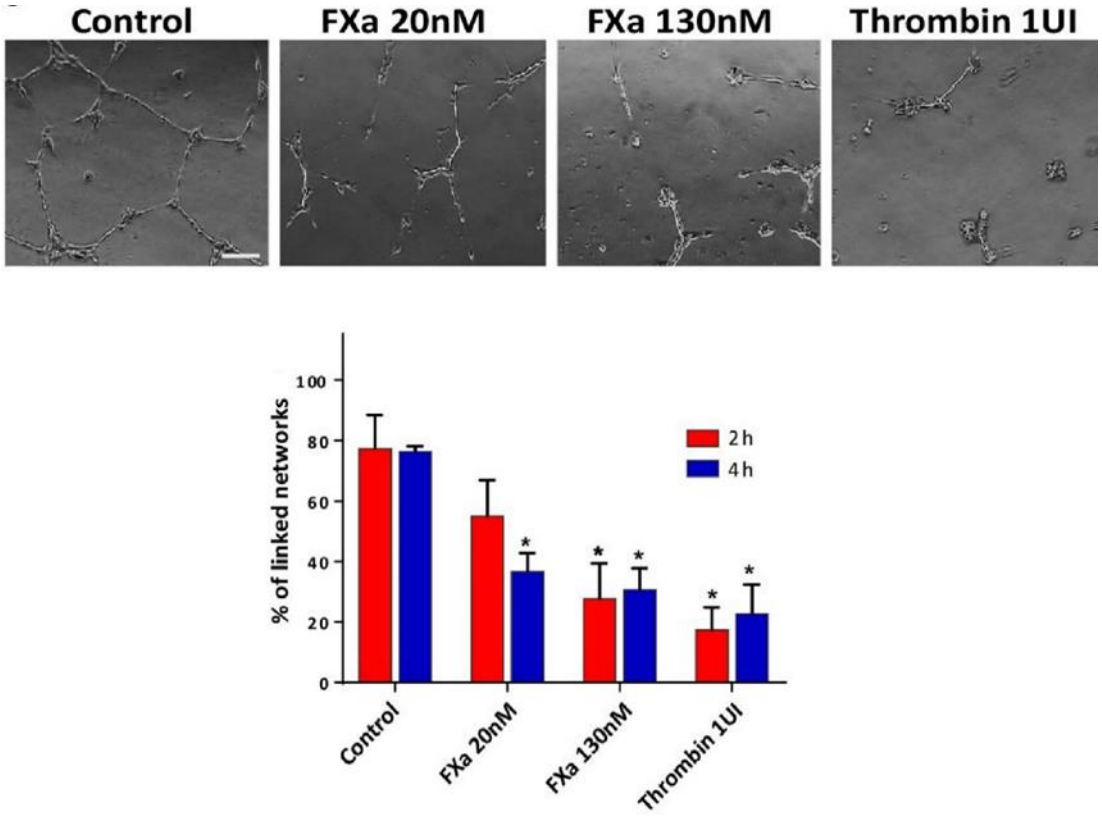

Figure 7. FXa disrupts tubular structures in Matrigel and promotes endothelial cell contraction. (A) HUVECs were seeded in Matrigel in the presence of VEGF (10ng/mL). 15 h later, FXa, in two different concentrations, was added to the tubular structures already formed. Images were taken and representative pictures in 10X are shown. (B) The contraction of this already formed tubular network was quantified 2 h (white bars) and 4 h (black bars) after FXa addition, n=4 $p<0.05$.

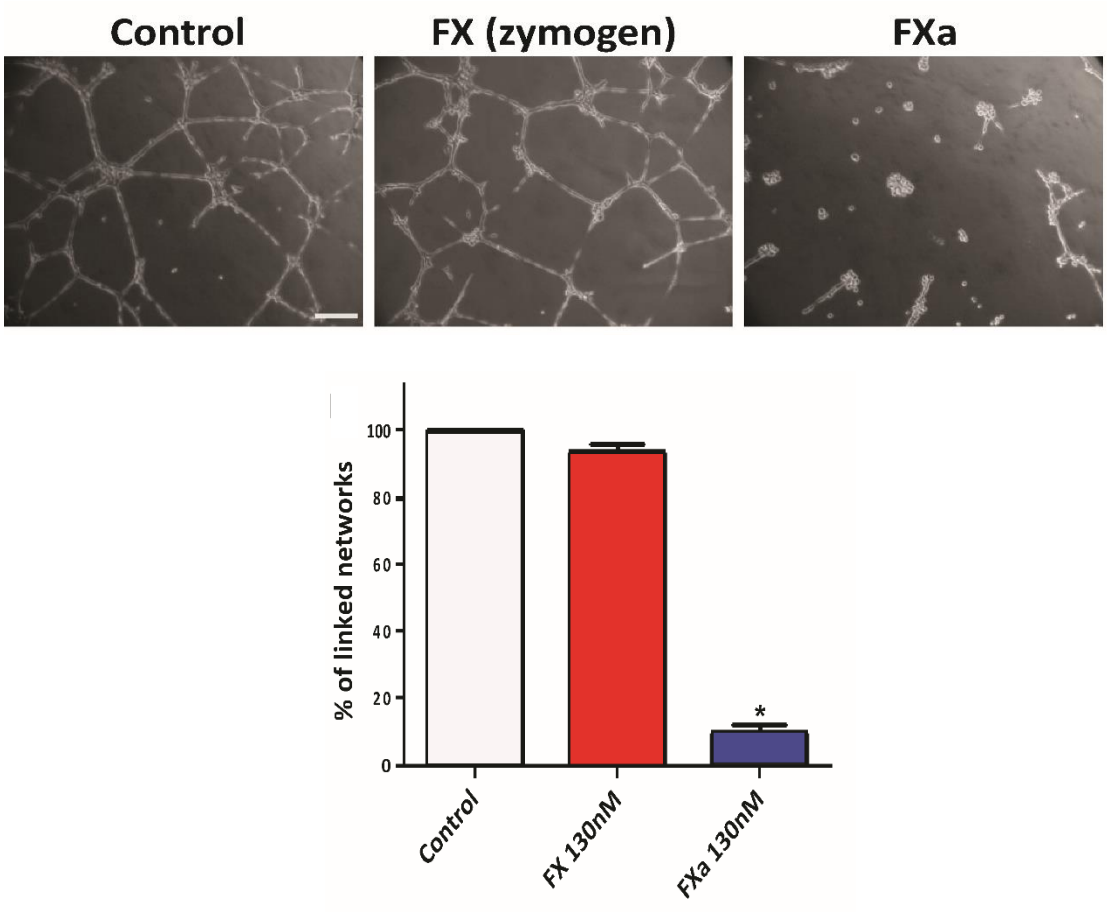

Figure 8. FXa, but not the zymogen, disrupts tubular structures formed by endothelial cells in Matrigel. EA.hy cells were seeded in Matrigel in the presence of VEGF (10ng/mL). 15 h later, FX (zymogen) or FXa were added to the tubular structures already formed. The disassembly of this established tubular network was evaluated after 4 h, using the master segments index from ImageJ software quantification tool, n=3 $p<0.05$.

5.5 FXa increases stress fiber formation and permeability-related protein responses in endothelial cells

Based on the finding suggesting that FXa is promoting endothelial cell contraction, we analyzed the F-actin stress fiber formation (indicator of cell contraction) in HUVEC seeded at high/low confluency. In a high-confluency state, F-actin-rich rings were present in control conditions; however, treatment with FXa promoted the loss of F-actin-rich rings and an increase in stress fiber formation throughout the monolayer (Fig 9A). Moreover, in a low-confluency state, there was a loss of lamellipodia at the leading edge and an increment in F-actin enriched stress fiber formation in response to FXa. Also, a decrease in the cell area was observed, suggesting that cell contraction was occurring (Fig 9B).

Additionally, the active form of RhoA (RhoA-GTP), a small GTPase identified as a regulator of the actin cytoskeleton and implicated in endothelial hyperpermeability, was observed in highly F-actin-enriched zones surrounding the edge of cell membrane in response to FXa treatment (Figure 10). The activation of this protein is related to cell contraction and cytoskeleton remodeling, suggesting that FXa is promoting a fast remodeling in endothelial cells.

Furthermore, phosphorylation of Focal Adhesion Kinase (pFAK, Y397), a protein involved in the assembly/disassembly of focal adhesions, was increased in response to FXa after 5 min of treatment (Fig 11). The Y397 phosphorylation site has been described as an essential autophosphorylation residue, which is one of the first targets of FAK activation, and thus promoting the down-stream phosphorylation of the other residues involved in the cellular response and cytoskeleton remodeling.

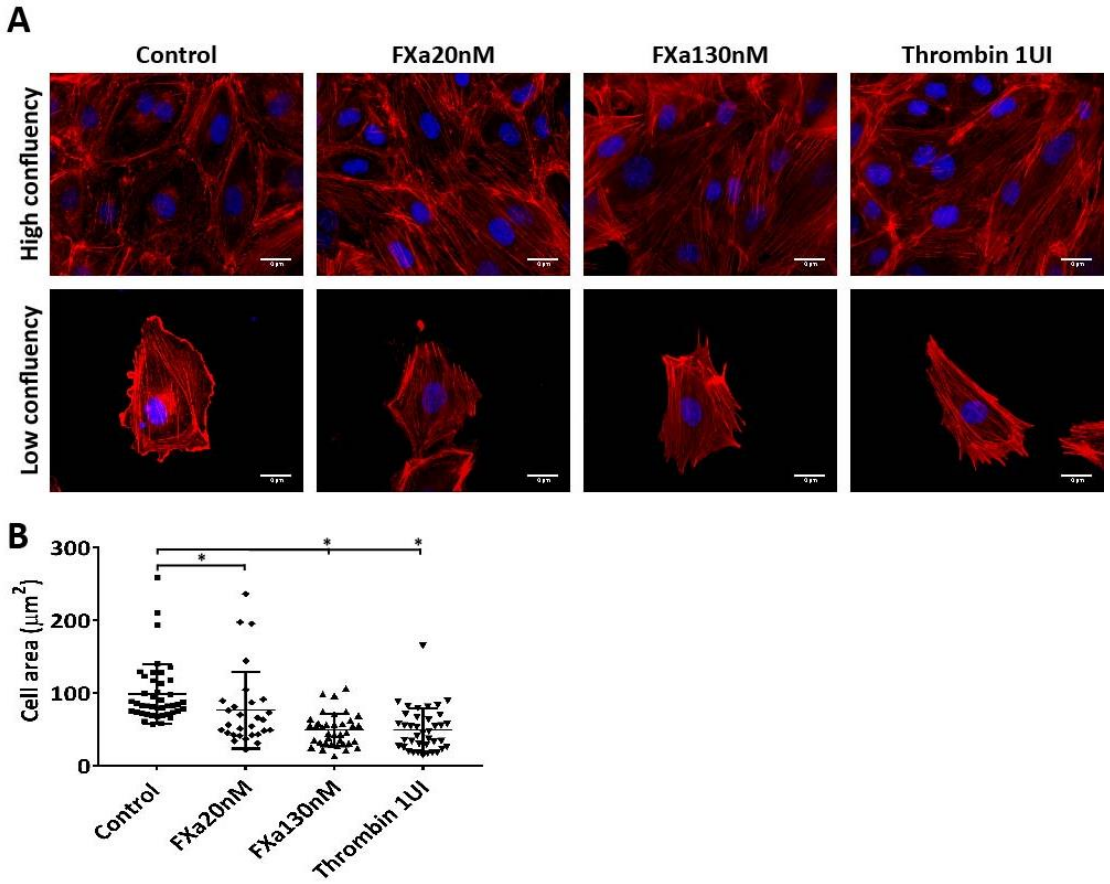

Figure 9. FXa promotes stress fiber formation and endothelial cell contraction (A) High/low confluency HUVECs were treated with FXa and thrombin, fixed and stained with Phalloidin-rhodamine to observe endothelial phenotype and stress fiber content. (B) Cell area was quantified using ImageJ software, $p<0.05$. Magnification bar = 10 µm

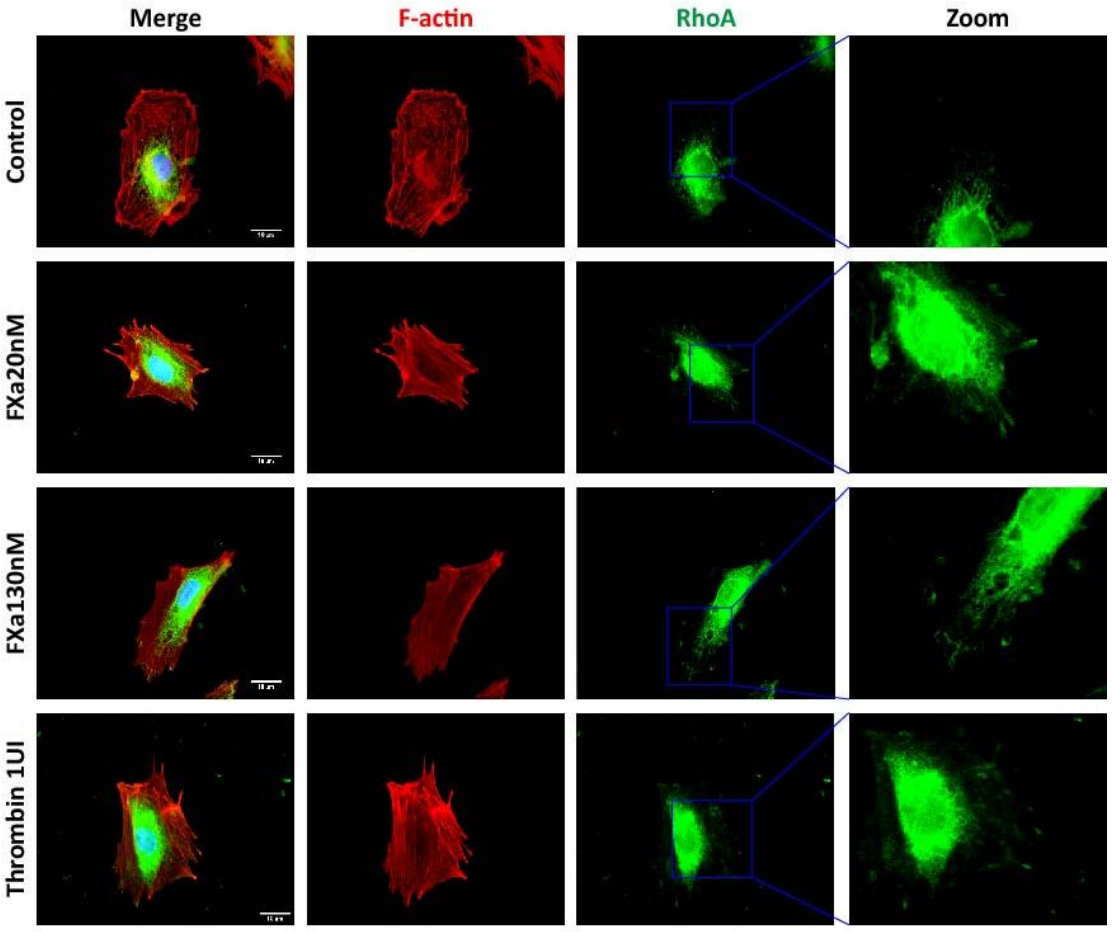

Figure 10. FXa-treatment promotes active RhoA localization at the edge of cells. HUVECs were treated for 5 min with FXa, fixed and prepared for the analysis of RhoA-GTP (active form) using the Far-IFI technique as described in methods. Stress fiber content was analyzed using Phalloidin-Rhodamine. Representative images at 100X are shown. Magnification bars in panels to the left = 10 μm.

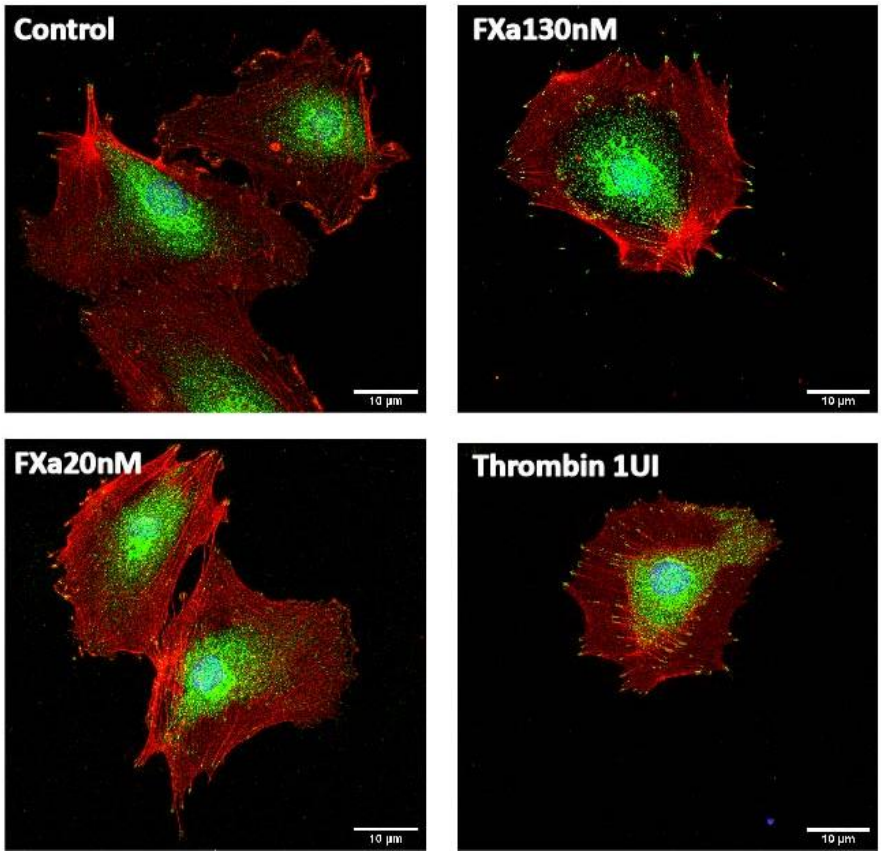

Figure 11. FXa promotes pFAK distribution to the cellular border. Endothelial cells were treated for 5 min with FXa, fixed and prepared for the analysis of the phosphorylated Focal Adhesion Kinase (pFAK, green stain) by Immunofluorescence. Stress fiber content was analyze using Phalloidin-Rhodamine. Representative images at 100X are shown. Magnification bar = 10 µm.

5.6 FXa induces endothelial hyperpermeability

Based on the previous results, in which FXa was triggering changes in the endothelial cytoskeleton and in cell-contraction related proteins, we assessed the effect of FXa on the permeability of an endothelial monolayer. First, FXa at both concentrations induced the disruption of an important member of adherent junctions family that controls endothelial permeability, VE-cadherin. The pattern distribution of VE-cadherin within a confluent HUVEC monolayer (Fig 12 A) and in the Human Pulmonary Microvasculature Endothelial cell line, HPMEC-1 (Fig 12 B) was disrupted in response to 30 min of FXa exposure, suggesting that FXa can change endothelial permeability. It is important to note that all these effects were due to FXa, as prothrombin or Thrombin were not present in this *in vitro* system.

The effect of FXa treatment on the permeability of an endothelial monolayer was evaluated using the Transwell system (Fig 13A). Briefly, endothelial cells were treated for 30 min with FXa, FX or Thrombin; and the permeability to the macromolecule BSA coupled to Evans Blue as a dye was evaluated. The pre-treatment with FXa, but not the zymogen FX, increased the permeability to Evans Blue-BSA (Figure 13B), as did also Thrombin (positive control).

This increase in endothelial permeability was maintained for at least 30 min.

After showing that FXa promotes endothelial hyperpermeability, we assessed the effect of FXa on vascular permeability to macromolecules *in vivo* using the cremaster model in C57BL/6 mice. The mice were anesthetized and the cremasteric muscle was exposed, prepared and treated topically with FXa (130nM). The mice were perfused with the macromolecule Dextran coupled with the green fluorescent molecule FITC to identify blood vessels and to analyze the extravasation of this dye. After 6 min of topical treatment, FXa significantly increased the FITC-

dextran extravasation to interstitial tissue (Fig 14), visible as an increase background fluorescence near of blood vessels.

5.7 An acute regime of FXa is enough to increase metastasis of B16F10

The aforementioned results suggest that FXa is increasing endothelial cell permeability, thus allowing circulating cancer cells to extravasate. Therefore, we hypothesized that FXa when applied only during the first 16h after cancer cell injection, when the cancer cells are attaching and crossing the endothelium into the pulmonary tissue, would result in increased metastasis 21 days later. Repeating the experiment detailed in figure 1, but now applying FXa only after injection of the cancer cells and /or 16h later (see schematic in Fig 15), we observed a clear increase in cancer metastasis at 21 days. In this case, we did not recreate the previous findings, in which FXa treatment increased the metastasis to different organs. Our results suggest that endothelial permeability is a potential mechanism by which FXa increases metastasis in this model.

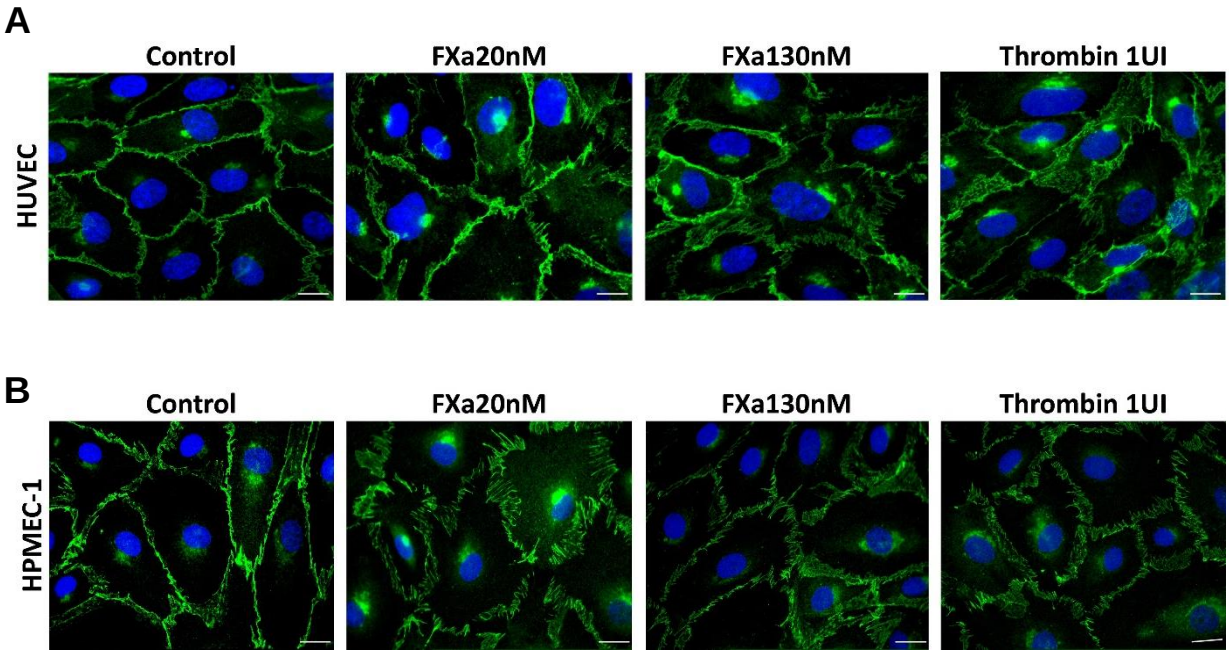

Figure 12. FXa promote VE-Cadherin disruption in HUVEC and in the Human Pulmonary Microvasculature Endothelial Cells, HPMEC-1. Distribution of VE-cadherin pattern was analyzed after 30 min of treatment with FXa and Thrombin as a positive control. Representative images at 100X amplification are shown. Magnification bars = 10 µm.

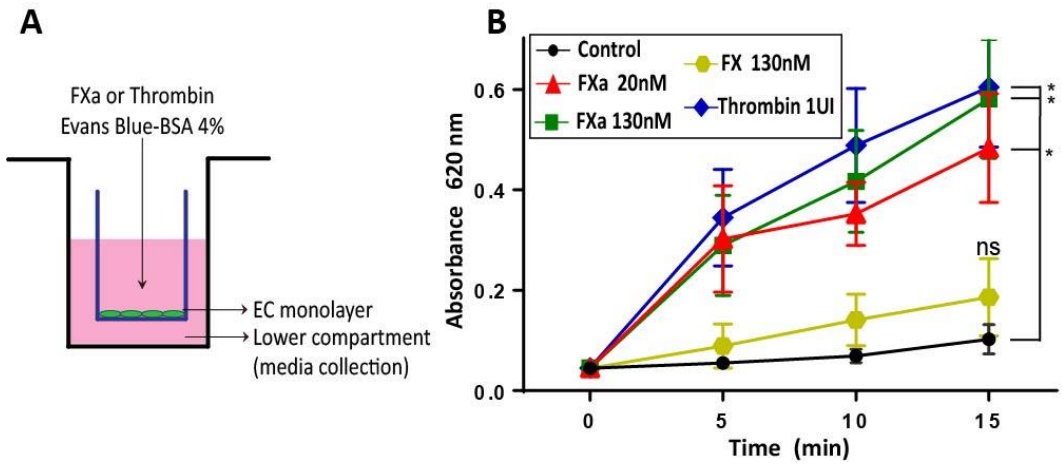

Figure 13. FXa induces endothelial hyperpermeability *in vitro*. (A) Endothelial cells were seeded onto 1% gelatin pre-coated Transwells (3µm) and allowed to proliferate until generating a 100% confluent monolayer. Cells were then treated with FXa or FX (zymogen) and thrombin for 30 min in serum free media (A). Evans Blue-BSA was added onto the upper chamber, and 100µL aliquots were taken from the lower chamber. (B) Evans Blue-BSA was measured as an indicator of hyperpermeability (Absorbance at 620nm) in time, n=5 $p<0.05$.

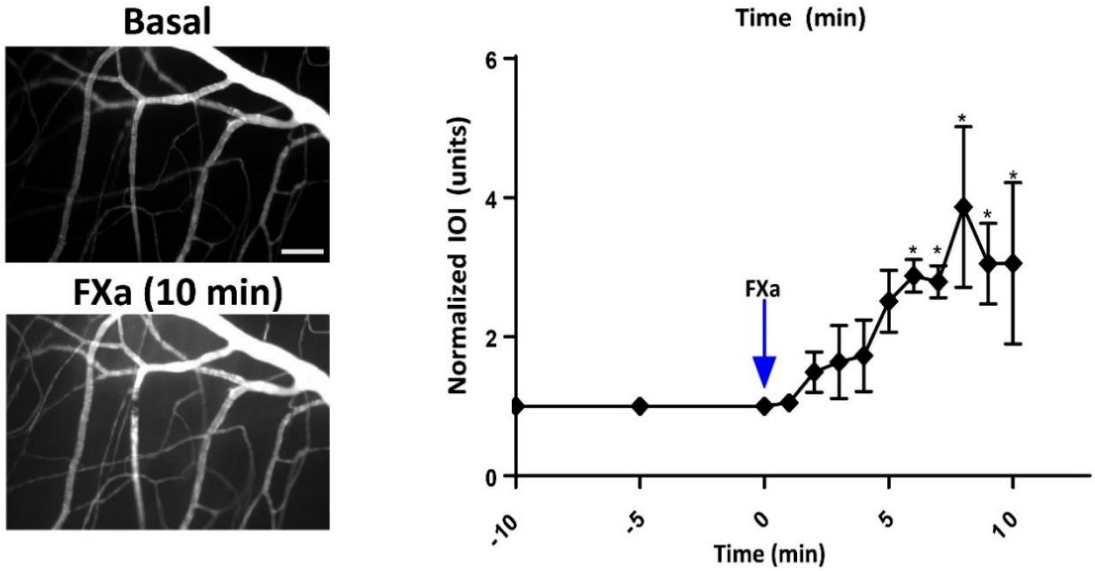

Figure 14. FXa induces endothelial hyperpermeability *in vivo*. Cremaster muscle from mice was exposed, prepared and treated topically with FXa. Vascular hyperpermeability to FITC-Dextran was evaluated using intravital microscopy and quantifying the integrated optical intensity (IOI) in the tissue for 10 min, n=3 $p<0.05$.

5.8 FXa changes mRNA expression within endothelial cells

Given the observed changes in the endothelial phenotype promoted by FXa, we assessed whether this was reflected in alterations at the transcriptional level using a GeneChip Human Gene 2.0 ST Array. After 4 h of treatment (EA.hy926 endothelial cell line), 127 genes were significantly up-regulated and 36 were down-regulated in response to FXa 130nM. These differences between treatments are represented in a heatmap (Fig 16A). A protein interaction network was generated based on the data from up-regulated genes and using the Gene Ontology Consortium database, showing a main cluster of proteins associated with the Interferon (IFN) response pathway. Transcripts of proteins associated with angiogenesis (FGF-2), inflammation (IL-6, ICAM-1), extracellular matrix degradation (PLAUR) and immune chemokines (CCL5) were also up-regulated in response to FXa (Fig 16B). In summary, the response triggered by FXa in endothelial cells matched to an inflammatory signature, validating the literature observations suggesting a role of the coagulation system in the inflammatory pathway. The entire list of up/down regulated genes is shown in Table 2 and 3 (Appendix).

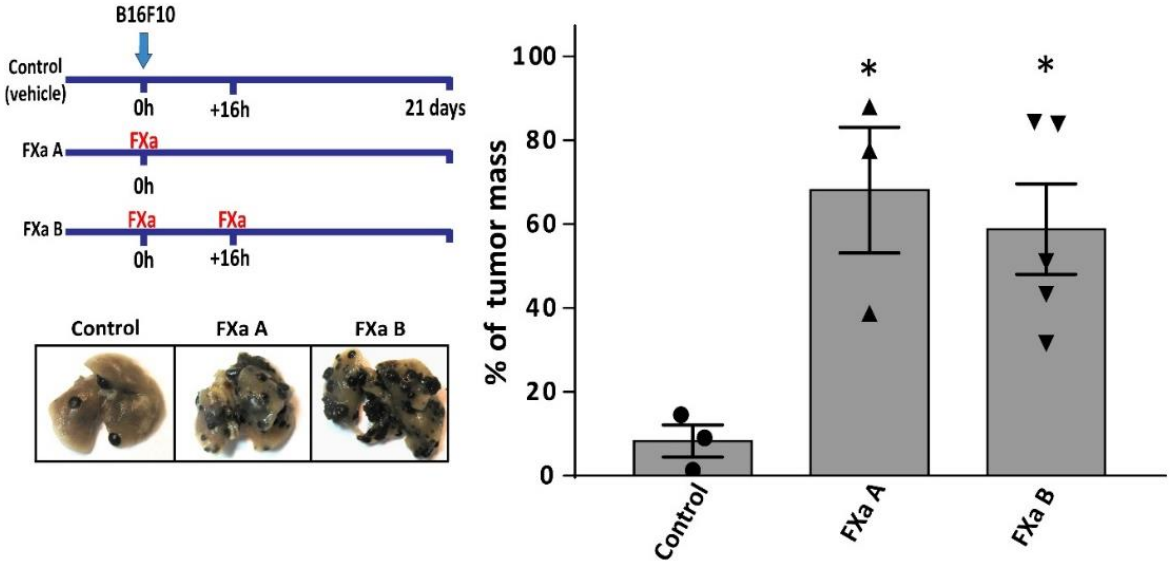

Figure 15. FXa increases metastasis in a short-term treatment. Schematic representation of the regimens of FXa administration in mice. FXa A & B groups were treated with FXa immediately after cancer cell injection but only FXa B group received a reinforcement 16h later. Representative images of lungs 21 days post-injection are shown and tumor mass referred to total lung mass was assessed.

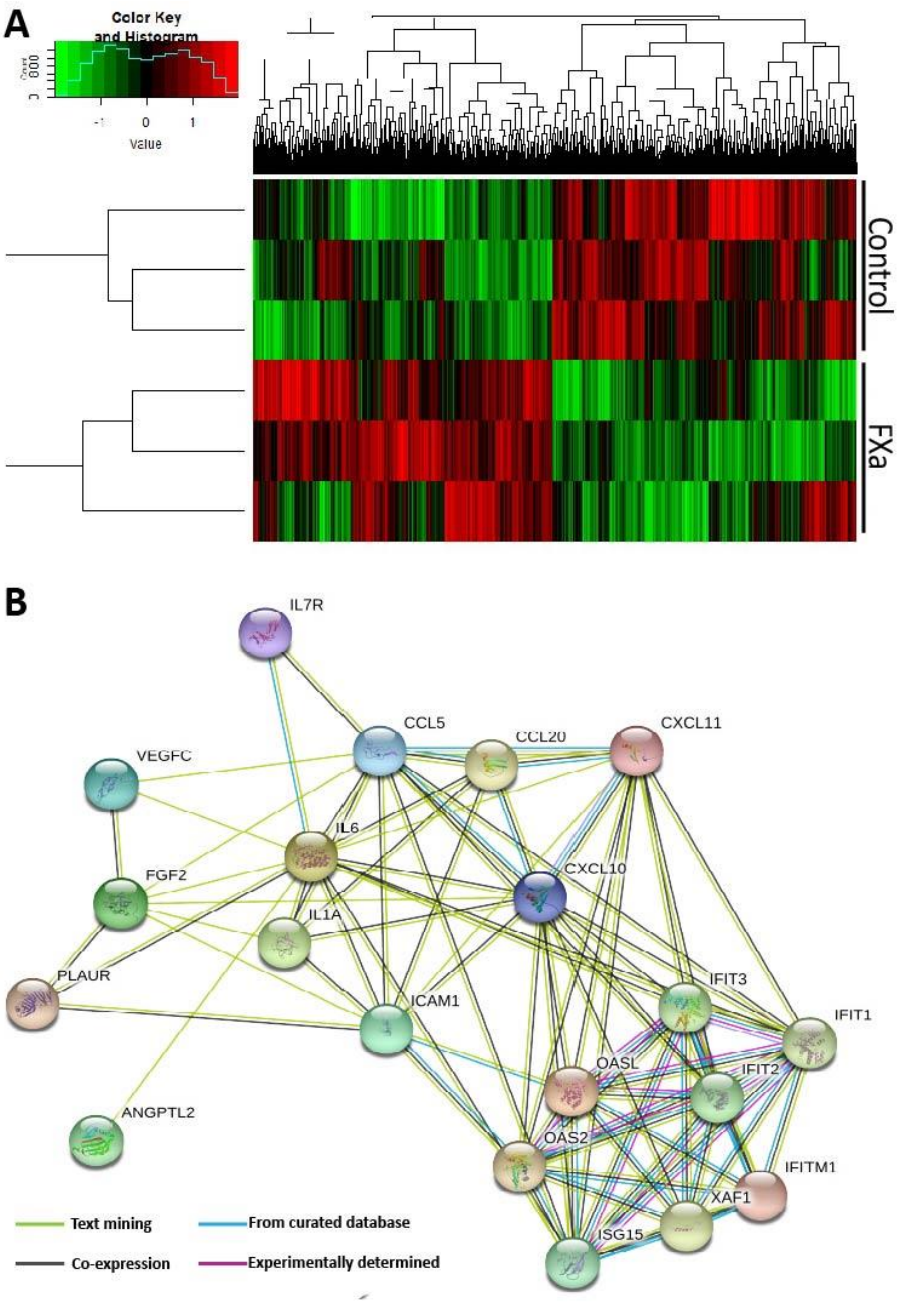

Figure 16. FXa induces changes in endothelial cell mRNA expression. (A) Gene expression signature of endothelial cells treated with FXa was evaluated with the Affymetrix Human Genome 2.0 ST Array. Heatmap shows the 6 analyzed samples (EA.hy control vs EA.hy treated with FXa130nM for 4h) clustered by condition at the left side of the image. Red and green colors represent up and downregulated genes respectively. Gene clusters are at the top of the heatmap. (B) Protein Interaction Network based on the top 10 Upregulated genes and some of our genes of interest. Further information on the main pathways involved in FXa treatment is shown in Table 1.

	Gene/Protein	Fold-change	Main reported functions
Top 5 up-regulated genes	IFI6 / Interferon alpha-inducible protein 6	10.7	Inhibition of apoptosis, INFs pathway
	IFIT2 / Interferon-induced protein with tetratricopeptide repeats 2	10	Inhibits expression of viral messenger RNA, INFs pathway
	IFIT1 / Interferon-induced protein with tetratricopeptide repeats 1	9.3	Inhibits growth and pathogenicity of some viruses, INFs pathway
	OAS2 / 2'-5'-oligoadenylate synthetase 2	8.8	Enzyme that activates RNAse L in response to viral infection, INFs pathway
	IFITM1 / Interferon-induced transmembrane protein 1	8	Membrane protein expressed in response to infections, INFs pathway
	CCL5 / RANTES	3.3	Chemotactic cytokine involved in monocytes, NK cells, memory T cells, eosinophils and Dendritic Cells recruitment
	FGF2 / Fibroblast Growth Factor 2	2.4	Potent proangiogenic factor, tumor promoting factor
	ICAM-1 / Intercellular Adhesion Molecule 1	2.4	Endothelial and leukocyte-associated transmembrane protein, involved in inflammatory response
	PLAUR / Plasminogen Activator Urokinase Receptor	1.5	Membrane receptor of Urokinase. Involved in fibrinolysis and extracellular matrix degradation/remodeling
	IL-6 / Interleukin-6	1.3	Pro-inflammatory cytokine, activates endothelial cells

Table 1. Top 5 up-regulated and top 5 "interesting" genes in response to FXa treatment in endothelial cells.

5.9 FXa increases lung immune infiltration, a process reverted by Dalteparin

To understand the contribution of FXa to inflammation *in vivo*, we analyzed the immune cell infiltration in lungs from mice treated with FXa alone or in combination with Dalteparin. In concordance with the microarray result, analysis of the non-cancer containing sections of the mice lungs showed that FXa treatment evoked an inflammatory response near blood vessels (Fig 17). As detected by the H&E stain, the immune infiltration was observed principally close to large blood vessels (based on the architecture, principally corresponding to veins and venules). This process was reversed or prevented by the presence of the anticoagulant Dalteparin, suggesting that anticoagulant treatment can have a potent anti-inflammatory effect.

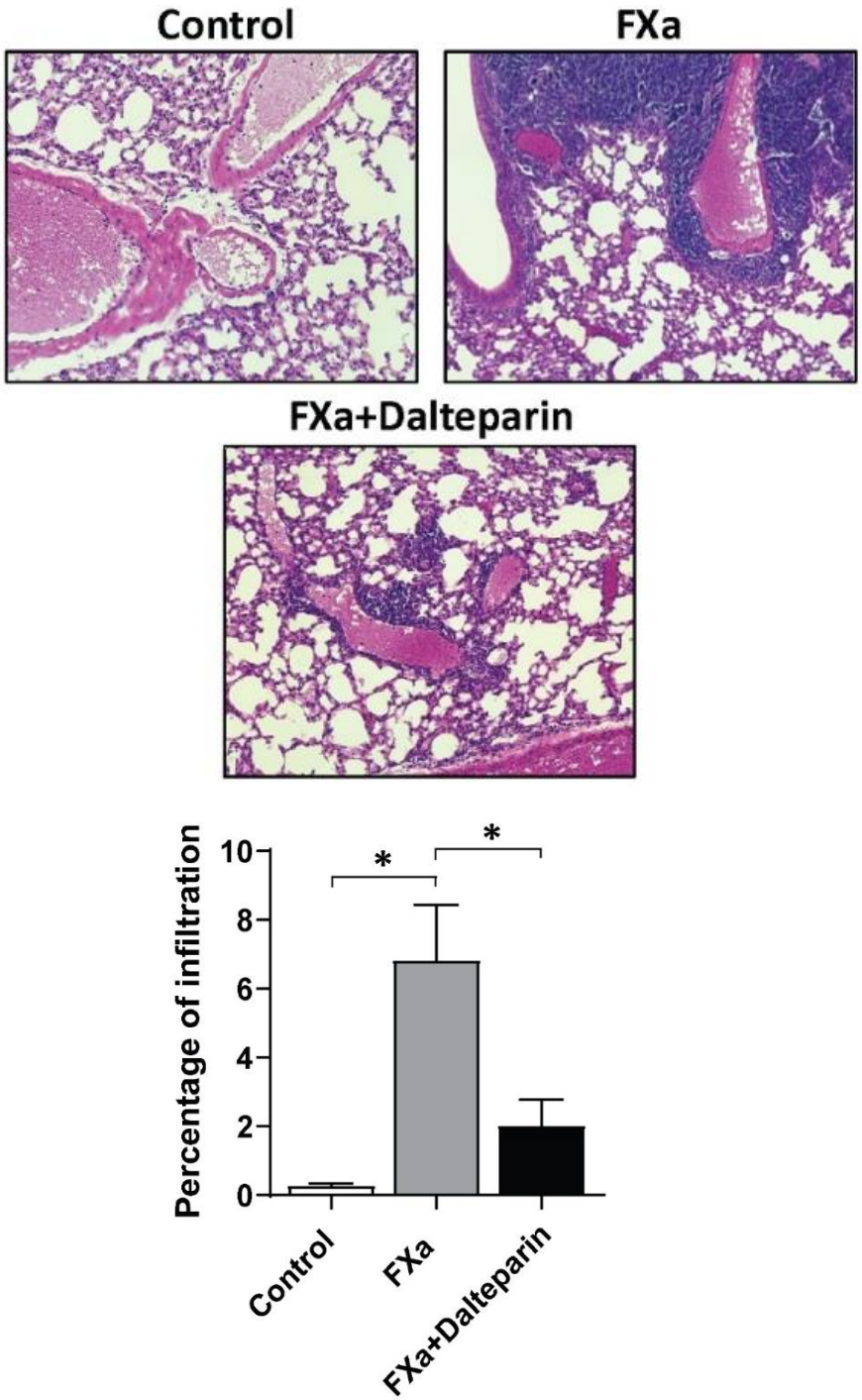

Figure 17. FXa treatment promotes a pro-inflammatory response in mice, an effect reduced by <u>Dalteparin treatment</u>. Lungs from mice treated with Vehicle, FXa and FXa+Dalteparin were stained with H&E to analyze immune cell infiltration. Immune infiltration was quantified and expressed as the percentage of total area per lung, $p<0.05$.

5.10 FXa increases cancer cell adhesion to the endothelium

Prior to cancer cell extravasation during metastasis, cancer cells must be attached firmly to the endothelium which allows them to withstand the pressure delivered by blood flow. As adhesion molecules allow cancer cell capture at the endothelial wall prior to extravasation, we assessed whether HUVEC increased adhesion molecules when treated with FXa. Figure 18 shows that FXa increased the protein levels of ICAM-1 and VCAM-1 after 4 and 8h of treatment. NO detectable levels were found at 2h post-treatment. Changes in VE-Cadherin total protein levels were not detected. Additionally, we also tested the response of the Human Pulmonary microvasculature Endothelial Cells (HPMEC-1) treated with FXa and Thrombin (as a positive control). We also used the monocyte cell line THP-1 treated with PMA as a control of ICAM-1 expression (Fig 19). We did not find statistical differences between cells treated with FXa, nevertheless we found statistical differences in the VCAM-1 levels of cells treated with Thrombin (Figure 19). A tendency to increased VCAM-1 total protein levels was observed in FXa-treated HPMEC-1, suggesting that Thrombin, instead of FXa, has a role in inflammation in this cell line.

As a proof of concept that FXa con enhance the adhesion of cancer cells to an endothelium, we pre-treated a confluent monolayer of HUVEC with FXa for 4h (Fig 20). After that, tumor cells (B16F10-eGFP) were added and co-incubated for 30 min, washed with warm PBS and fixed for visualization. There was a significant increase in the number of attached B16F10-eGFP cancer cells to endothelial cells treated with FXa and Thrombin under static conditions (Fig 21).

Interestingly, to assess the increase in adhesion under “physiological” conditions, we used a microfluidic microchannel, where B16F10 cells were pumped over a FXa pre-treated HUVEC

monolayer. In line with our previous experiment, we observed that under flow conditions FXa increased adhesion of B16F10 to endothelial cells (Fig. 20).

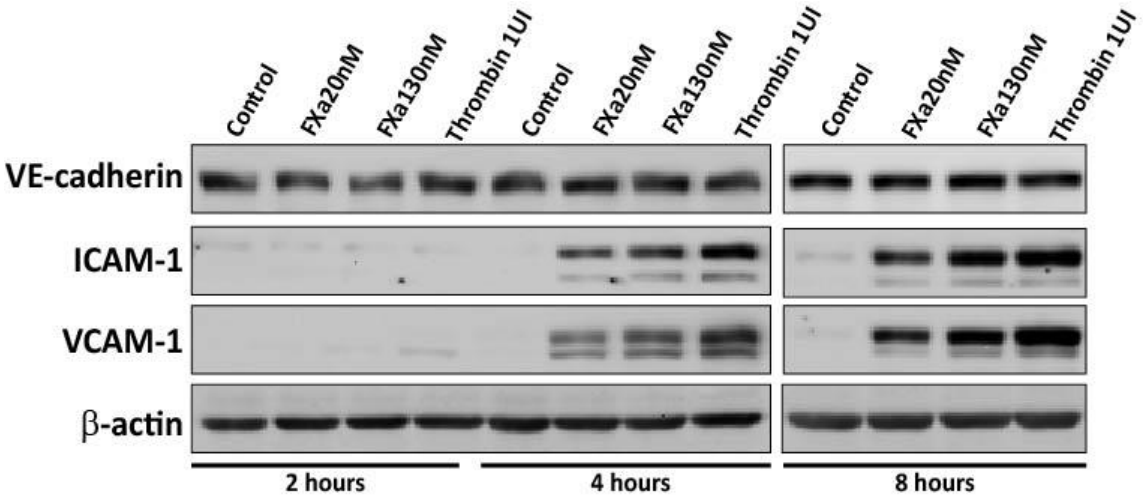

Figure 18. FXa promotes adhesion molecule expression in HUVEC. 100% confluent HUVECs were treated with thrombin, FXa or vehicle in no serum media and total protein levels of the adhesion molecules ICAM-1 and VCAM-1 were analyzed. Representative images of 4 independent HUVEC primary cultures are shown.

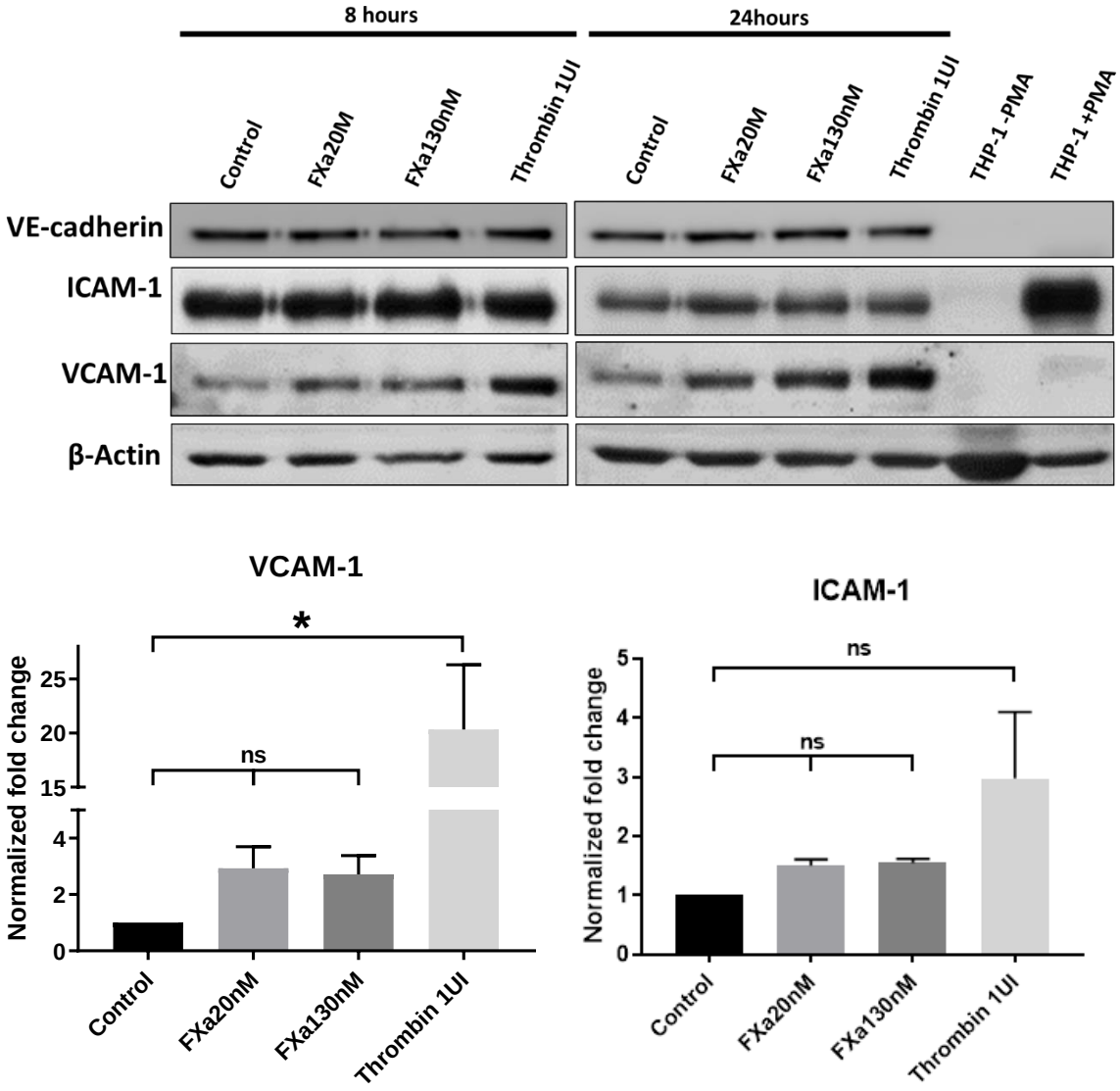

Figure 19. Thrombin, but not FXa, increases ICAM-1 protein levels in HPMEC-1. 100% confluent HPMEC-1 cells were treated with thrombin, FXa or vehicle in no serum media and total protein levels of the adhesion molecules ICAM-1 and VCAM-1 were analyzed. Representative images of 4 independent HUVEC primary cultures are shown. Quantification of normalized relative levels is shown.

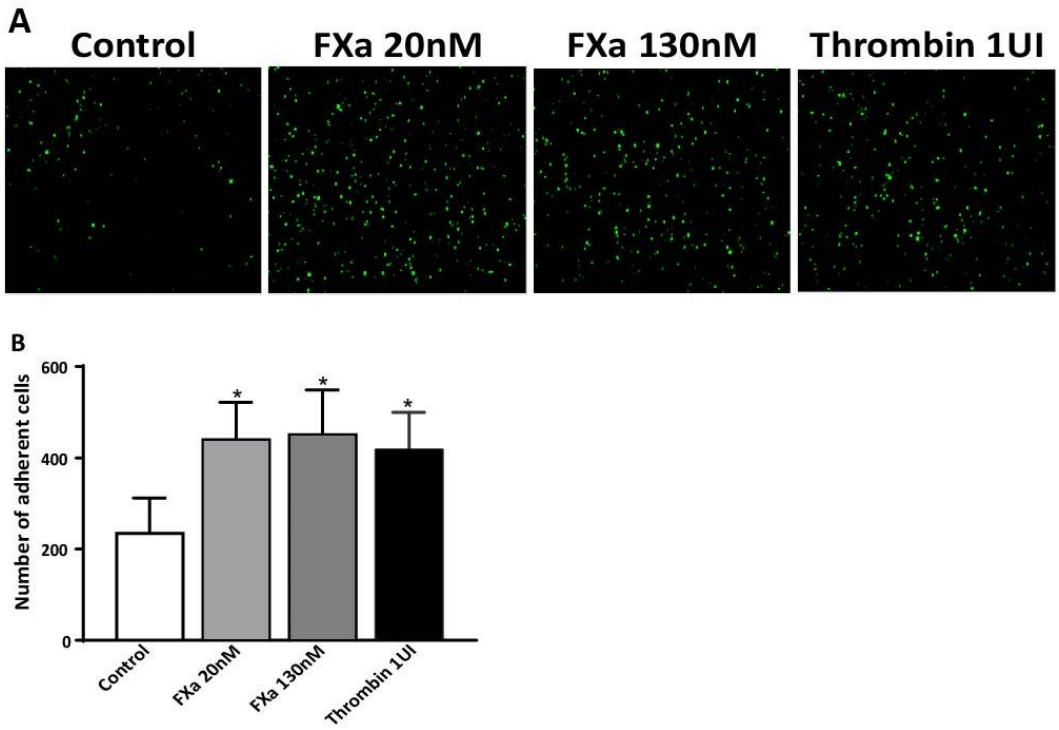

Figure 20. FXa and Thrombin increases the adhesion of B16F10 under static conditions. (A) B16F10-eGFP cells were seeded for 30 min over a confluent monolayer of HUVEC cells pretreated with either vehicle or FXa for 4h. Subsequently, cells were washed with warm PBS, fixed and mounted for visualization. The number of B16F10-eGFP cells that remained attached were determined by fluorescence microscopy and using the particle counter of ImageJ software. n=4 $p<0.05$.

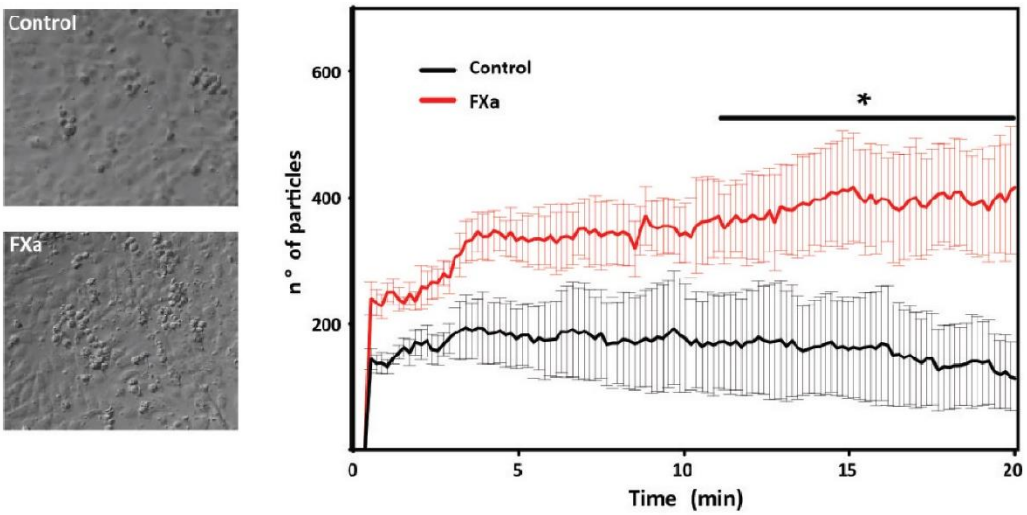

Figure 21. FXa increases the adhesion of B16F10 under flow conditions.
A microfluidic adhesion assay was developed, where HUVEC cells were treated for 6h with either control or FXa (130nM) prior to underflow conditions (flow 50µL/min, 37°C and 5% CO_2), delivering 175.000 B16F10 cells per min. Resulting adherent cells were evaluated with live imaging for 20 min and then quantified using ImageJ software n=3 $p<0.05$.

Taking in consideration that FXa elicited an inflammatory response over endothelial cells, and thus promoting cancer cell adhesion, our next objective was to relate these findings to clinical observations. To assess that, we performed an analysis of the ICAM-1 and VCAM-1 ligands transcripts levels in melanoma patients using the TCGA-TIMER database. Consistent with an important role of the cell adhesion molecules ICAM-1 and VCAM-1 in melanoma metastasis, we observed that there is a significant increase of the adhesion molecules ligands: ITGAL, ITGAM, ITGB1, ITGB2 and ITGA4 mRNA levels in metastasis samples in comparison to primary tumor samples (Fig 22). This result suggests that melanoma cells that express these adhesion molecule ligands could have an advantage to metastasize, thus promoting their clonal expansion and maintaining the expression of molecules that facilitate the metastatic process.

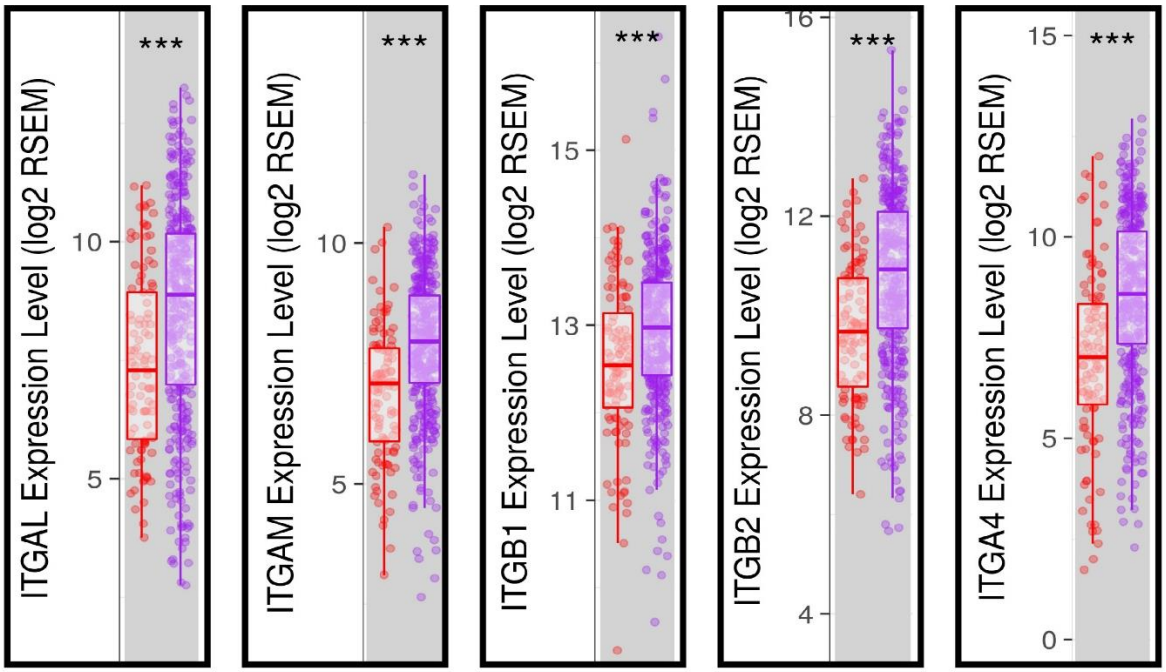

Figure 22. RNA levels of adhesion molecule <u>ligands</u> are increased in metastasis samples compared to primary tumors. ICAM-1 ligands (LFA-1 and MAC-1) and VCAM-1 (VLA-4) were analyzed using TCGA-TIMER database to evaluate the relative RNA expression of endothelial adhesion molecules ligands (red boxplot represents primary tumors from melanoma patients, mine while purple boxplots represent metastasis samples). Data was extracted from 333 primaries and 331 metastatic melanomas patients (https://cistrome.shinyapps.io/timer/).

6 DISCUSSION

Given the suggested association between the anticoagulant treatment and cancer progression we wished to determine if alterations in the coagulation system changed the level and distribution of cancer cell metastasis. To this end we utilized the syngeneic model of metastasis, the B16F10 murine melanoma in C57BL/6 mice. Melanoma cells were injected into the tail vein followed by the intravenous administration of either vehicle, zymogen FX or FXa. The administration of intravenous coagulation factors in mouse models has been reported previously to study inflammation (Kondreddy et al., 2018). The physiological concentration of the zymogen FX is reported to be in the range of 130nM (Palta et al., 2014). Experimentation *in vitro* has suggested that the concentration of FXa generated from TF microvesicles and acting upon a substrate is in the range of 10-50nM. While the zymogen has a half-life of 40h, FXa half-life is only believed to be min due to inactivation by circulating serine protease inhibitors, such as antithrombin II (Bunce et al., 2011). Thus, in our animal models we added a higher concentration (130 nM) of FXa in the tail vein injection to have a prolonged enzymatic effect upon the lungs of the experimental mouse model (B16F10 produces primarily lung metastasis). Several *in vivo* models have been established to study the importance of the coagulation cascade and the relation to other diseases, in which the majority uses vein occlusion as the promoter of coagulation cascade and thrombus formation (Albadawi et al., 2017). The concept of FXa intravenous introduction, applied in the study presented herein, was to create a hypercoagulable environment in a healthy animal and preliminary experiments with this concentration of FXa demonstrated that this dose was well tolerated, with no adverse side effects or animal deaths being observed.

A recognized relationship between the coagulation system and cancer progression is now in its second century of investigation, yet the exact participation of the coagulation factors in the metastatic process is still poorly understood. The publications generated in hematology suggest that the coagulation factors possess yet-to-be-defined functions upon the intact endothelium and in tumor microenvironment. Herein, we present evidence that activated coagulation factor Xa can promote melanoma metastasis and thus open the door to the evaluation of direct FXa inhibitors in the exclusive setting of cancer metastasis. Moreover, we present evidence that the action of FXa is not upon the cancer cell, but in fact upon the vascular endothelium, resulting in changes in adhesion molecule expression and hyperpermeability, thus potentially promoting the process of extravasation (metastasis). Interestingly, the use of anticoagulants has long been associated with improved cancer patient outcome, potentially through the decrease of thrombotic events (Gerotziafas et al., 2008); however the positive non-hemostatic effect of an anticoagulant regime has not yet been addressed. Despite the FRAGMATIC trial using the preferential FXa inhibitor Dalteparin in cancer patients being established to evaluate this, no beneficial action upon cancer patient survival was observed (Griffiths et al., 2009). However, in this trial we hypothesize that lack of a beneficial effect was because most of enrolled patients had already presented metastasis. Thus, a possibly beneficial effect of the anticoagulant over cancer metastasis and progression may have been lost or diluted out from the study. After half a century of cancer investigation it is now clear that every cancer stage is unique, and the same compound may promote or inhibit cancer progression depending on the cancer stage. Three oral FXa inhibitors: Apixaban, Rivaroxaban and Edoxaban, have passed clinical trials and are US Food and Drug Administration approved for the treatment of VTE in cancer patients. A potential anti-cancer effect of these second-generation anticoagulants is under evaluation. However, as

we hypothesize that the coagulation cascade leading to a blood clot is independent of the action of coagulation factors upon the endothelium, it is a possibility that anticoagulants, such as apixaban, rivaroxaban or dabigatran (thrombin inhibitor) may have differing effects upon cancer metastasis than the results we observed with Dalteparin. A recent publication has reported that neither rivaroxaban or dabigatran reduce metastasis *in vivo* mouse models (Buijs et al., 2019).

The non-hemostatic effect of coagulation proteases (such as: FVIIa, FXa, Thrombin and Activated Protein C) are intimately linked to PAR-1 and PAR-2 signaling. These receptors are widely expressed among several cell types and trigger different responses. As an example, Thrombin increase permeability over an endothelial monolayer, a process dependent of RhoA activation and Ca^{+2} signaling (van Nieuw et al., 2000), contrary to the anti-inflammatory and barrier-protective effect of Activated Protein C triggered also by PAR-1 cleavage (de Ceunynck et al., 2018). Furthermore, platelet activation (through PAR-1 cleavage) allows the attachment to the endothelium via von Willebrand Factor-GPIb interaction, causing the release of several molecules that regulate wound healing and inflammation (Golebiewska and Poole, 2015). The binding of coagulation proteases to the PARs receptors is regulated by conserved regions like the Gla domain and EGF like domains. Interestingly, Feistritzer and collaborators proposed that FXa has a barrier-protective role in endothelial monolayers through PAR-1 and -2 activation (Feistritzer et al., 2005), a process dependent on the binding to the endothelial protein C receptor (Schuepbach et al., 2010). On the other hand, a recent study shows that FXa leads to increase intracellular Ca^{2+} and NF-κβ levels in endothelial cells (Artim-Esen et al., 2017), supporting our observation, in which FXa has a proinflammatory effect. Moreover, morphological and functional observations i*n vivo* and *in vitro* suggest that FXa, independently of Thrombin, have anti-angiogenic properties over vein-derived (HUVEC) endothelial cells and this is mediated by

PAR-1, but not PAR-2 (Lange et al., 2014). Recently, it has been proposed that alterations in the permeability of the endothelium occur in response to the activation of PAR-2 by FXa in arterial and microvascular cells *in vitro* and this is independent of the TF /FVIIa complex (Benelhaj et al., 2019). While we clearly demonstrate specific actions of FXa in *in vitro*/*in vivo* models and we show an effect of the predominantly FXa inhibitor Dalteparin over metastasis, our study has caveats. Although our *in vitro* FXa experiments were performed in the absence of prothrombin and Thrombin, certain cancer promoting effects of FXa *in vivo* may contain a contribution from Thrombin. This possibility is hard to control. The zymogen FX (endotoxin free) that was isolated under the same methodology and applied in an identical manner did not demonstrate activity in our experiments. Given the dual and potentially independent action of coagulation factors upon endothelial permeability and coagulation, the use of exclusive thrombin-inhibitors or other anticoagulants may independently affect cancer metastasis. Experiments are currently ongoing to address this issue and determine the role of the new generation of anticoagulants in this melanoma metastasis model. Despite the uncertainty that the increase in cancer metastasis may be aided in part by Thrombin generation, our work clearly shows that activation of the coagulation system promotes metastasis, and this can be reduced by a first-line treatment anticoagulant such as the predominantly FXa-inhibitor Dalteparin.

Chronic inflammation is a known contributor to metastasis and inflammatory cells have been shown to contribute to the pre-metastatic niche (Liu et al., 2016). Moreover, molecules such as Histamine, TNF-α, Lipopolysaccharide (LPS), are known to promote endothelial hyperpermeability and adhesion molecule exposure, suggesting a potent role over cancer metastasis (Pober and Sessa, 2007). As an example, LPS exposure, and consequential inflammatory response, results in increased B16F10 lung metastasis (Tang et al., 2018). Herein,

we demonstrate by microarray analysis that pro-inflammatory signals are enhanced within the endothelium upon FXa exposure and this was confirmed by increased immune cell infiltration in FXa-treated mouse lungs. In accordance with our results, other authors have reported elevated IL-6 and IL-8 release from HUVEC in response to FXa. Promisingly, Dalteparin reduced immune cell infiltration into the lung, offering another potentially beneficial clinical action of this drug (Natoni et al., 2016). Using a similar model, reduced leukocyte infiltration into mouse lung was observed by other authors upon the intravenous introduction of the coagulation factor VIIa after prior exposure to LPS (Kondreddy et al., 2018). Whether the increase in lung metastasis observed by FXa in our model is an effect of an inflammatory response or occurs as a consequence of tumor cell invasion will be part of future experiments and investigation. However, this result clearly demonstrates the association between the coagulation cascade activation, endothelial activation, inflammation and metastasis.

Interestingly, the cancer promoting action of this coagulation factor was not restricted to metastasis. We demonstrate that the presence of FXa increased the growth of solid tumors in two distinct immunocompromised mice models injected with human cell lines. While in this paper we concentrated on the role of FXa upon the endothelial activation, and the potential increase in metastasis due to enhanced extravasation, it did not escape our intention that the presence of FXa on a continual basis caused a greater increase in lung tumor mass in the B16F10 model than that brought about by initial dosage. This may suggest, and hopefully future experiments will demonstrate, that FXa also provides a growth advantage to already established tumor masses of B16F10 cells, whether it be in the mouse lung or flank. As we observed no effect of FXa upon biological actions of cancer cells (Figure 4 & 5), we can speculate that the inflammatory environment enhanced by FXa is promoting tumor growth and/or there is a

promotion of vascular growth to irrigate the tumor mass. Additionally, the pro-metastatic effect of FXa could be elicited by a physiological mechanisms evoked by this protease in the mice vasculature, similarly to physiological mechanisms of immune cell extravasation and tissue invasion in a damaged tissue.

In summary, in our mouse models, increased circulating FXa promotes tumor burden and melanoma metastasis.

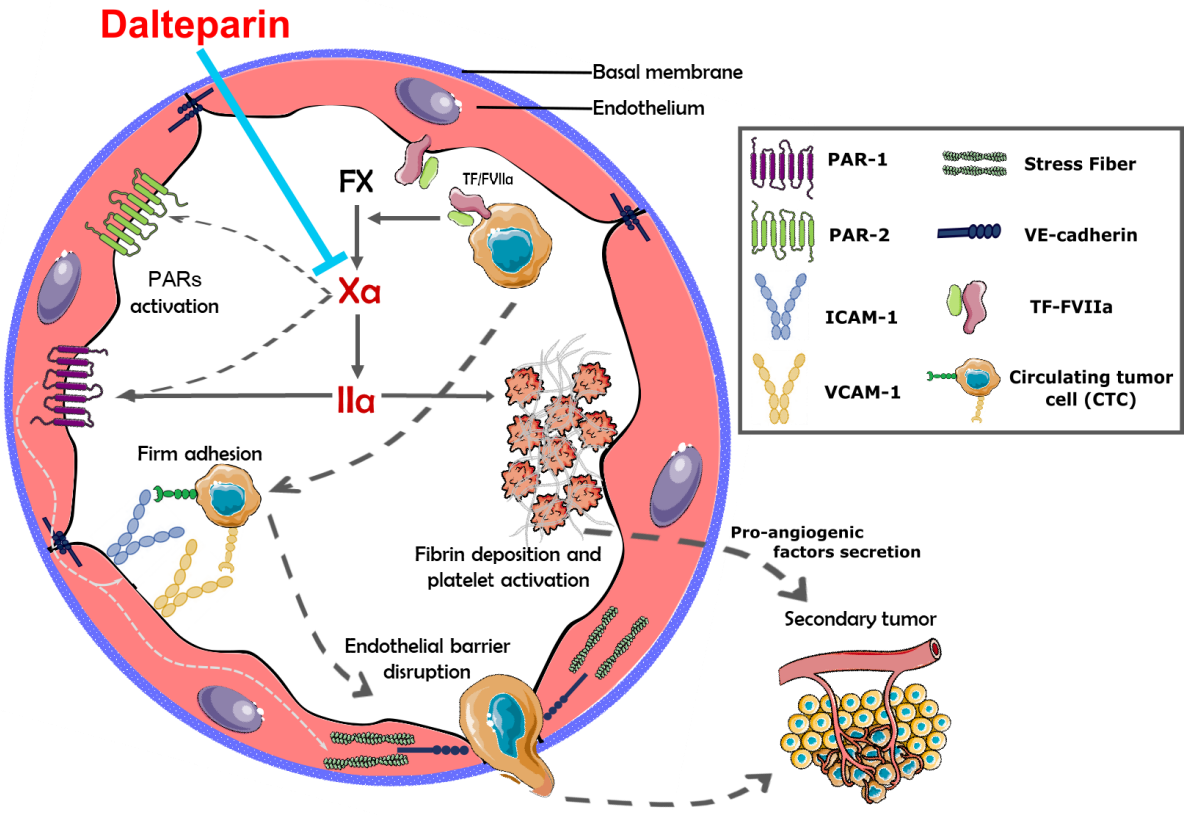

Figure 23. Proposed model to FXa action upon endothelial cell and consequently increases circulating tumor cell metastasis.

7 CONCLUSIONS AND PROJECTIONS

Based on the increasing evidence that link the thrombosis to cancer progresion, we showed that the central protease of the coagulation pathway, FXa, has a non-haemostatic role over endothelial cells by promoting the metastasis of melanoma cells. Additionally, the influence of FXa (independently of Thrombin) on endothelial activation and in the inflammatory response was demostrated. Taking together, our data suggest that the mechanism of action by which FXa is increasing metastasis involves a direct effect upon endothelial cells, increasing ICAM and VCAM, leading to enhanced adhesion of cancer cells to the endothelium. Additionally, FXa potentially increased extravasation due to an increase in cytoskeletal rearrangement and endothelial hyperpermeability. No evidence was found related to a direct effect of FXa over cancer cells. This work, together with limited information from literature, suggest beneficial effects of anticoagulant treatment, especially Dalteparin and low-molecular-weight heparins, in the setting of metastatic melanoma disease. We propose that future trials should have the premise that not all anticoagulants will have the same outcomes, nor will all stages of the malignant process show a beneficial response to anticoagulant treatment. This and other approaches may finally deliver a beneficial clinical application to Armand Trousseau's 1865 observation that cancer and hypercoagulability are connected.

8 REFERENCES

Albadawi, A.A. Witting, Y. Pershad, A. Wallace, A.R. Fleck, P. Hoang, A. Khademhosseini, R. Oklu, Animal models of venous thrombosis, Cardiovasc. Diagn. Ther. (2017) 197–206.

Altinbas, H.S. Coskun, O. Er, M. Ozkan, B. Eser, a Unal, M. Cetin, S. Soyuer, A randomized clinical trial of combination chemotherapy with and without low-molecular-weight heparin in small cell lung cancer., J. Thromb. Haemost. 2 (2004) 1266–71.

Artim-Esen, N. Smoktunowicz, T. McDonnell, V.M. Ripoll, C. Pericleous, I. MacKie, E. Robinson, D. Isenberg, A. Rahman, Y. Ioannou, R.C. Chambers, I. Giles, Factor Xa Mediates Calcium Flux in Endothelial Cells and is Potentiated by Igg from Patients with Lupus and/or Antiphospholipid Syndrome, Sci. Rep. (2017) 10788-10795.

Bendas, L. Borsig, Cancer cell adhesion and metastasis: Selectins, integrins, and the inhibitory potential of heparins, Int. J. Cell Biol. 2012 (2012).

Benelhaj, A. Maraveyas, S. Featherby, M.E.W. Collier, M.J. Johnson, C. Ettelaie, Alteration in endothelial permeability occurs in response to the activation of PAR2 by factor Xa but not directly by the TF-factor VIIa complex, Thromb. Res. (2019) 238-247.

Borensztajn, M.P. Peppelenbosch, C.A. Spek, Coagulation Factor Xa inhibits cancer cell migration via LIMK1-mediated cofilin inactivation, Thromb. Res. 125 (2010) 323–328.

Buijs, E.H. Laghmani, R.F.P. van den Akker, C. Tieken, E.M. Vletter, K.M. van der Molen, J.J. Crooijmans, C. Kroone, S.E. Le Dévédec, G. van der Pluijm, H.H. Versteeg, The Direct Oral Anticoagulants Rivaroxaban and Dabigatran do not Inhibit Orthotopic Growth and Metastasis of Human Breast Cancer in Mice, Thromb. Res. (2019).

Bunce, R. Toso, R.M. Camire, Zymogen-like factor Xa variants restore thrombin generation and effectively bypass the intrinsic pathway in vitro, Blood. (2011) 290-298.

Bustos, O. Lucchesi, M.C. Ruete, L.S. Mayorga, C.N. Tomes, Rab27 and Rab3 sequentially regulate human sperm dense-core granule exocytosis, Proc. Natl. Acad. Sci. (2012) 2057-2066.

De Ceunynck, C.G. Peters, A. Jain, S.J. Higgins, O. Aisiku, J.L. Fitch-Tewfik, S.A. Chaudhry, C. Dockendorff, S.M. Parikh, D.E. Ingber, R. Flaumenhaft, PAR1 agonists stimulate APC-like endothelial cytoprotection and confer resistance to thromboinflammatory injury, Proc. Natl. Acad. Sci. (2018) 982-991.

Desch, C. Gebhardt, J. Utikal, S.W. Schneider, D-dimers in malignant melanoma: Association with prognosis and dynamic variation in disease progress, Int. J. Cancer. 140 (2017) 914–921.

Durán, A. Seyama, K. Yoshimura, D.R. González, P.I. Jara, X.F. Figueroa, M.P. Borić, Stimulation of NO production and of eNOS phosphorylation in the microcirculation in vivo, Microvasc. Res. (2000) 104-11.

Ebrahimi, F. Rahmani, R. Behnam-Rassouli, F. Hoseinkhani, M.R. Parizadeh, M.R. Keramati, M. Khazaie, A. Avan, S.M. Hassanian, Proinflammatory signaling functions of thrombin in cancer, J. Cell. Physiol. 232 (2017) 2323–2329.

Elyamany, A.M. Alzahrani, E. Bukhary, Cancer-associated thrombosis: An overview, Clin. Med. Insights Oncol. 8 (2014) 129–137.

Erices, S. Cubillos, R. Aravena, F. Santoro, M. Marquez, R. Orellana, C. Ramírez, P. González, P. Fuenzalida, M.L. Bravo, B. Oliva, S. Kato, C. Ibañez, J. Brañes, E. Bravo, C. Alonso, K. García, C. Arab, V.A. Torres, A.S. Godoy, J. Pereira, G. Bustos, J.C. Cardenas, M.A. Cuello, G.I. Owen, Diabetic concentrations of metformin inhibit platelet-mediated ovarian cancer cell progression, Oncotarget. (2017) 20865-20880.

Falanga, M. Marchetti, A. Vignoli, Coagulation and cancer: Biological and clinical aspects, J. Thromb. Haemost. 11 (2013) 223–233.

Feistritzer, R. Lenta, M. Riewald, Protease-activated receptors-1 and -2 can mediate endothelial barrier protection: Role in factor Xa signaling, J. Thromb. Haemost. 3 (2005) 2798–2805.

Ferjancic, A.M. Gil-Bernabé, S.A. Hill, P.D. Allen, P. Richardson, T. Sparey, E. Savory, J. McGuffog, R.J. Muschel, VCAM-1 and VAP-1 recruit myeloid cells that promote pulmonary metastasis in mice., Blood. 121 (2013) 3289–3297.

Gerotziafas, C. Papageorgiou, M. Hatmi, M.-M. Samama, I. Elalamy, Clinical studies with anticoagulants to improve survival in cancer patients., Pathophysiol. Haemost. Thromb. 36 (2008) 204–211.

Golebiewska, A.W. Poole, Platelet secretion: From haemostasis to wound healing and beyond, Blood Rev. (2015) 153-162.

Griffiths, S. Burns, S.I. Noble, F.R. Macbeth, D. Cohen, T.S. Maughan, FRAGMATIC: A randomised phase III clinical trial investigating the effect of fragmin® added to standard therapy in patients with lung cancer, BMC Cancer. 9 (2009) 355-364.

Haddad, E.W. Greeno, Chemotherapy-induced thrombosis, Thromb. Res. 118 (2006) 555–568. Han, K. Jin, K. He, J. Cao, L. Teng, Protease-activated receptors in cancer: A systematic review, Oncol. Lett. 2 (2011) 599–608.

Henriquez, C. Calderon, M. Quezada, B. Oliva, M.L. Bravo, E. Aranda, S. Kato, M.A. Cuello, J. Gutierrez, A.F.G. Quest, G.I. Owen, Progesterone utilizes distinct membrane pools of tissue factor to increase coagulation and invasion and these effects are inhibited by TFPI, J. Cell. Physiol. 226 (2011) 3278–3285.

Kakkar, M.N. Levine, Z. Kadziola, N.R. Lemoine, V. Low, H.K. Patel, G. Rustin, M. Thomas, M. Quigley, R.C.N. Williamson, Low molecular weight heparin, therapy with dalteparin, and survival in advanced cancer: The fragmin advanced malignancy outcome study (FAMOUS), J. Clin. Oncol. 22 (2004) 1944–1948.

Kasthuri, M.B. Taubman, N. Mackman, Role of tissue factor in cancer, J. Clin. Oncol. 27 (2009) 4834–4838.

Kirwan, C.N. Mccollum, G. Mcdowell, G.J. Byrne, Investigation of Proposed Mechanisms of Chemotherapy-Induced Venous Thromboembolism: Endothelial Cell Activation and Procoagulant Release Due to Apoptosis, in: Clin. Appl. Thromb. (2015) 420-427.

Kolaczkowska, P. Kubes, Neutrophil recruitment and function in health and inflammation, Nat. Rev. Immunol. 13 (2013) 159–75.

Kondreddy, J. Wang, S. Keshava, C.T. Esmon, L. Vijaya Mohan Rao, U.R. Pendurthi, Factor VIIa induces anti-inflammatory signaling via EPCR and PAR1, Blood. (2018) 2379-2392.

Krupiczojc, C.J. Scotton, R.C. Chambers, Coagulation signalling following tissue injury: Focus on the role of factor Xa, Int. J. Biochem. Cell Biol. (2008) 1228–1237.

Lampugnani, E. Dejana, Adherens junctions in endothelial cells regulate vessel maintenance and angiogenesis, Thromb. Res. 120 (2007) 1–6.

Lange, I. Gonzalez, M.P. Pinto, M. Arce, R. Valenzuela, E. Aranda, M. Elliot, M. Alvarez, S. Henriquez, E. V. Velasquez, F. Orge, B. Oliva, P. Gonzalez, M. Villalon, K.M. Cautivo, A.M. Kalergis, K. Pereira, C. Mendoza, C. Saez, S. Kato, M.A. Cuello, F. Parborell, G. Irusta, V. Palma, M.L. Allende, G.I. Owen, Independent Anti-Angiogenic Capacities of Coagulation Factors X and Xa, J. Cell. Physiol. (2014) 1673-1680.

Laresche, F. Pelletier, F. Garnache-Ottou, T. Lihoreau, S. Biichlé, G. Mourey, P. Saas, P. Humbert, E. Seilles, F. Aubin, Increased levels of circulating microparticles are associated with increased procoagulant activity in patients with cutaneous malignant melanoma, J. Invest. Dermatol. 134 (2014) 176–182.

Läubli, L. Borsig, Selectins as Mediators of Lung Metastasis, Cancer Microenviron. 3 (2010) 97–105.

Liu, X. Cao, Characteristics and Significance of the Pre-metastatic Niche, Cancer Cell. (2016) 668-681.

Muhsin-Sharafaldine, S.C. Saunderson, A.C. Dunn, J.M. Faed, T. Kleffmann, A.D. McLellan, Procoagulant and immunogenic properties of melanoma exosomes, microvesicles and apoptotic vesicles, Oncotarget. 7 (2016) 324-330.

Muñoz. Martín, I. Ortega, C. Font, V. Pachón, V. Castellón, V. Martínez-Marín, M. Salgado, E. Martínez, J. Calzas, A. Rupérez, J.C. Souto, M. Martín, E. Salas, J.M. Soria, Multivariable clinical-genetic risk model for predicting venous thromboembolic events in patients with cancer, Br. J. Cancer. 118 (2018) 1056–1061.

Natoni, M.S. Macauley, M.E. O'Dwyer, Targeting Selectins and Their Ligands in Cancer, Front. Oncol. 6 (2016) 1–12.

Nguyen, P.D. Bos, J. Massagué, Metastasis: from dissemination to organ-specific colonization., Nat. Rev. Cancer. 9 (2009) 274–284.

Noble, J. Pasi, Epidemiology and pathophysiology of cancer-associated thrombosis, Br. J. Cancer. 102 (2010) 2–9.

Oyarce, S. Cruz-Gomez, F. Galvez-Cancino, P. Vargas, H.D. Moreau, N. Diaz-Valdivia, J. Diaz, F.A. Salazar-Onfray, R. Pacheco, A.M. Lennon-Dumenil, A.F.G. Quest, A. Lladser, Caveolin-1 expression increases upon maturation in dendritic cells and promotes their migration to lymph nodes thereby favoring the induction of CD8+ T cell responses, Front. Immunol. (2017).

Palta, Saroa R, Palta A, Overview of the coagulation system, Indian J. Anaesth. (2014) 515-523.
Patterson, R.A. Rhoades, J.G. Garcia, Evans blue dye as a marker of albumin clearance in cultured endothelial monolayer and isolated lung., J. Appl. Physiol. 72 (1992) 865–73.
Pober, W.C. Sessa, Evolving functions of endothelial cells in inflammation, Nat Rev Immunol. 7 (2007) 803–815.

Reymond, B.B. D'Água, A.J. Ridley, Crossing the endothelial barrier during metastasis., Nat. Rev. Cancer. 13 (2013) 858–70.
Schuepbach, M. Riewald, Coagulation factor Xa cleaves protease-activated receptor-1 and mediates signaling dependent on binding to the endothelial protein C receptor, J. Thromb. Haemost. (2010) 379-388.

Senden, T.M. Jeunhomme, J.W. Heemskerk, R. Wagenvoord, C. van't Veer, H.C. Hemker, W.A. Buurman, Factor Xa induces cytokine production and expression of adhesion molecules by human umbilical vein endothelial cells, J Immunol. 161 (1998) 4318–4324.

Sparsa, H. Durox, V. Doffoel-Hantz, E.M. Munyangango, C. Bédane, J. Cendras, C. Gantois, S. Boulinguez, J.M. Bonnetblanc, High prevalence and risk factors of thromboembolism in stage IV melanoma, J. Eur. Acad. Dermatology Venereol. 25 (2011) 340–344.

Tang, Q.Y. Cao, X.Y. Guo, S.H. Dong, J.A. Duan, Q.N. Wu, Q.L. Liang, Inhibition of p38 and ERK1/2 pathways by Sparstolonin B suppresses inflammation-induced melanoma metastasis, Biomed. Pharmacother. (2018) 382-389.

Torres-Estay, D. Carreño, P. Fuenzalida, A. Watts, I.F. San Francisco, P.C. Sotomayor, J. Ebos, G.J. Smith, A.S. Godoy, Androgens modulate male-derived endothelial cell homeostasis using androgen receptor-dependent and receptor-independent mechanisms, Angiogenesis. 20 (2016) 25–38.

van Nieuw Amerongen, S. Van Delft, M.A. Vermeer, J.G. Collard, V.W.M. van Hinsbergh, Activation of RhoA by Thrombin in Endothelial Hyperpermeability: Role of Rho Kinase and Protein Tyrosine Kinases, Circ. Res. (2000) 335-340.

Vestweber, VE-cadherin: The major endothelial adhesion molecule controlling cellular junctions and blood vessel formation, Arterioscler. Thromb. Vasc. Biol. 28 (2008) 223–232.

Zamorano, N. Marín, R. Carrasco, P. Mujica, F.G. González, C. Quezada, C.J. Meininger, M.P. Boric, W.N. Durán, F.A. Sánchez, S-Nitrosation of β-catenin and p120 catenin: A novel regulatory mechanism in endothelial hyperpermeability, Circ. Res. 111 (2012) 553–563.

Zigler, T. Kamiya, E.C. Brantley, G.J. Villares, M. Bar-Eli, PAR-1 and thrombin: The ties that bind the microenvironment to melanoma metastasis, Cancer Res. 71 (2011) 6561–6566

9 APPENDIX

Table 2. List of up-regulated genes in response to a 4h-treatment with FXa over endothelial cells.

Differentially Expressed Genes of EA.hy926 treated cells							
127 Up regulated Coding Genes							
Row	**Symbol**	**logFC**	**FC**	**AveExpr**	**t**	**P.Value**	**adj.P.Val**
7118	IFI6	3.42173209	10.7162786	3.55444326	13.9858144	2.02E-05	0.00649445
7122	IFIT2	3.33592662	10.0975026	0.65915951	62.6259109	6.99E-09	6.40E-05
7120	IFIT1	3.22259681	9.33465571	0.63502608	50.1913022	2.28E-08	7.27E-05
10508	OAS2	3.15298438	8.89493693	0.84011287	41.5142986	6.30E-08	0.00014301
7125	IFITM1	3.00947807	8.05273057	0.8626442	40.5374149	7.15E-08	0.00014301
7123	IFIT3	2.98607781	7.92317027	0.79084727	37.9268818	1.02E-07	0.00014368
17431	XAF1	2.76254815	6.78593755	0.70702777	71.3325308	3.48E-09	6.38E-05
10510	OASL	2.7135008	6.55911331	0.77708491	39.8324213	7.85E-08	0.00014301
7469	ISG15	2.33110796	5.03191641	1.02365572	33.5546328	1.96E-07	0.00024405
7320	IL7R	2.08876151	4.25382745	0.78343804	54.7064475	1.44E-08	6.59E-05
3965	DDX58	2.06915647	4.19641242	1.8791801	12.4078729	3.78E-05	0.01047377
3968	DDX60	2.06672637	4.18934986	1.45437695	30.1155842	3.49E-07	0.00037596
6668	HERC6	1.9862985	3.96219121	1.17880823	23.7851472	1.23E-06	0.00085575
7117	IFI44L	1.98364121	3.95489999	0.60067419	33.4338573	2.00E-07	0.00024405
13593	SAMD9L	1.96174325	3.89532379	1.93138261	19.3064869	3.70E-06	0.00193757
13592	SAMD9	1.94745162	3.85692641	3.08570053	15.3660145	1.23E-05	0.00461229
10507	OAS1	1.92966877	3.80967721	1.0214498	27.5076191	5.66E-07	0.00047064
7116	IFI44	1.92006052	3.78438934	1.06104245	57.4152416	1.11E-08	6.59E-05
12510	PTGS2	1.8363912	3.57115611	1.12545947	25.8594553	7.86E-07	0.00062542
11190	PARP9	1.80560581	3.4957592	1.02769166	18.4557942	4.70E-06	0.00232595
10509	OAS3	1.74690793	3.35638435	0.80857095	14.9335591	1.43E-05	0.00504896
6667	HERC5	1.74170981	3.34431285	0.38981481	49.7962158	2.38E-08	7.27E-05
2463	CCL5	1.70444702	3.25903991	0.62784876	22.0220936	1.84E-06	0.0010893
7119	IFIH1	1.69198829	3.23101687	0.456204	29.2663753	4.07E-07	0.00041353
2451	CCL20	1.6891635	3.22469676	0.45640049	41.9289734	5.97E-08	0.00014301
11845	PMAIP1	1.67532146	3.19390512	1.84596686	13.7728908	2.19E-05	0.00679853
3677	CXCL11	1.59446991	3.01983538	0.36587973	39.0888197	8.68E-08	0.00014301
17606	ZC3HAV1	1.59063529	3.01181945	1.91084544	16.2114351	9.32E-06	0.00370718
16406	TRANK1	1.49804718	2.82460119	0.60239613	22.4462799	1.67E-06	0.00101724
16219	TNFAIP3	1.48562038	2.80037567	0.78323591	15.2904357	1.27E-05	0.00463864
11182	PARP14	1.47727625	2.78422586	1.76741398	27.9253753	5.22E-07	0.00045503
4395	DTX3L	1.44583286	2.72420044	2.03869701	24.1731968	1.12E-06	0.00082349
13507	RTP4	1.29091809	2.44683715	0.40757651	23.2478768	1.38E-06	0.00090466
7115	IFI35	1.24449237	2.36935171	1.06787932	23.6538149	1.26E-06	0.00085575
5456	FGF2	1.24218013	2.36555733	3.37379725	13.9917717	2.02E-05	0.00649445
7079	ICAM1	1.24189899	2.3650964	0.75299424	15.3830168	1.23E-05	0.00461229
10057	NFKBIA	1.20445511	2.30450214	1.46890806	9.77409513	0.00012928	0.02572549
3640	CTSS	1.17869264	2.26371548	1.37251767	17.4257516	6.37E-06	0.00277487
16854	UBE2L6	1.15918432	2.23331123	0.94845573	16.4348555	8.67E-06	0.00352609
15880	TLR3	1.12374377	2.17911717	1.48643314	16.7181912	7.92E-06	0.00334152
3969	DDX60L	1.12102838	2.17501957	2.09808543	10.5068331	8.92E-05	0.02022566

2741	CEACAM1	1.11149267	2.16069085	1.10175107	8.60782018	0.00024646	0.03709546
14778	SP110	1.09246219	2.1323765	1.08656554	14.8740033	1.46E-05	0.00505865
13594	SAMHD1	1.07762997	2.11056604	2.70092666	25.3072905	8.81E-07	0.00067227
7271	IL1A	1.05556042	2.07852546	0.69472206	11.1391281	6.60E-05	0.01656214
5906	GBP4	1.04179979	2.05879444	0.3017827	38.5334907	9.37E-08	0.00014301
17151	VEGFC	0.98690784	1.98193252	1.28160437	10.9647026	7.16E-05	0.01725848
5920	GCH1	0.96777187	1.95581766	0.68380665	28.7045847	4.51E-07	0.00042599
15126	STAT1	0.96191635	1.9478956	3.03926836	19.6588936	3.37E-06	0.0018125
3061	CLDN1	0.96117159	1.94689029	0.87703279	9.32523294	0.0001643	0.02857813
10202	NOCT	0.95275951	1.93557137	1.06663208	8.32866261	0.00029095	0.04050646
16462	TRIM22	0.95265346	1.9354291	2.14815241	15.3845612	1.23E-05	0.00461229
7111	IFI27	0.92621715	1.90028677	0.63304574	15.0187365	1.39E-05	0.00499657
6520	H1F0	0.89047636	1.85378812	2.00570835	12.0143403	4.46E-05	0.01184452
8172	KYNU	0.87893559	1.83901799	1.21033178	16.6744652	8.03E-06	0.00334152
13931	SFR1	0.87104306	1.82898476	1.75961866	9.22104696	0.00017396	0.02921654
821	APOL6	0.86049425	1.81566022	0.78929092	17.5381755	6.15E-06	0.00274772
7891	KITLG	0.83475228	1.78355077	1.34824045	9.68686355	0.00013534	0.02615647
10062	NFKBIZ	0.81689605	1.76161181	0.68955735	13.6294169	2.31E-05	0.00697218
1265	B2M	0.79052444	1.72970313	3.1978479	8.32728878	0.00029119	0.04050646
13416	RPS6KC1	0.77672601	1.71323851	0.93438994	11.2083207	6.40E-05	0.01626356
18245	ZNFX1	0.75115401	1.68313863	2.62128538	7.97415465	0.00036178	0.0438621
4869	ERRFI1	0.7491879	1.68084641	2.86229851	12.1690131	4.18E-05	0.01141424
5608	FNDC3A	0.73661693	1.66626392	2.58932158	8.6512256	0.00024028	0.03696535
4604	EIF2AK2	0.73628388	1.66587931	2.52430654	8.27055561	0.00030136	0.04050646
7150	IFNL1	0.70479934	1.62991795	0.26070624	19.8117454	3.23E-06	0.00179242
16521	TRIML2	0.6985838	1.6229109	1.96231954	8.155485	0.00032329	0.04082849
7453	IRF9	0.68699757	1.60992956	0.46256241	9.68503623	0.00013547	0.02615647
14520	SLFN5	0.66707341	1.58784865	2.02505062	9.81913565	0.00012628	0.02555484
723	ANPEP	0.66630611	1.58700438	3.33386294	9.46220955	0.00015254	0.02746005
7110	IFI16	0.65111957	1.57038638	3.20243785	9.61573575	0.00014053	0.0265824
7279	IL1RL1	0.64623177	1.56507497	0.64824137	7.68069458	0.0004361	0.04958846
11725	PLAUR	0.62992438	1.54748388	2.59412064	9.4566861	0.000153	0.02746005
1153	ATP1B1	0.58431057	1.49932233	2.85612474	8.47313351	0.00026684	0.03825004
9882	NCF2	0.58365285	1.49863895	0.27068826	17.8250556	5.65E-06	0.00258527
7144	IFNB1	0.57103515	1.48558911	0.22182637	21.82275	1.94E-06	0.00110741
10505	OAF	0.54925069	1.46332547	0.67575253	8.74156715	0.00022801	0.03594105
8216	LAP3	0.54378787	1.45779501	1.07471916	8.19610243	0.00031534	0.04082849
7470	ISG20	0.5420519	1.45604193	0.37770354	10.5269693	8.84E-05	0.02022566
7583	JUNB	0.52951613	1.44344499	0.76438506	9.13584781	0.00018235	0.0300542
13458	RSAD2	0.52191911	1.435864	0.19773224	28.5336397	4.65E-07	0.00042599
11181	PARP12	0.51103536	1.42507254	1.433799	8.49965712	0.00026268	0.03816519
2892	CFLAR	0.50917809	1.42323914	0.52972008	8.28903826	0.000298	0.04050646
4824	ERAP2	0.5081923	1.42226698	1.02025916	10.0826387	0.00011027	0.02283314
1383	BCL6	0.5019877	1.41616337	1.1049534	7.65238982	0.00044418	0.04988676
15127	STAT2	0.48321352	1.39785384	0.60707519	11.0877357	6.76E-05	0.01673314
3676	CXCL10	0.476501	1.39136506	0.19390125	22.4594907	1.66E-06	0.00101724
5903	GBP1	0.47140155	1.38645573	0.24262444	12.6618567	3.40E-05	0.00970443
17781	ZNF185	0.45792845	1.37356811	1.7192309	9.80778406	0.00012703	0.02555484
1449	BIRC3	0.45412224	1.36994906	0.22507888	17.9114877	5.51E-06	0.00258527
7316	IL6	0.45352557	1.36938258	0.40782373	8.46937587	0.00026744	0.03825004

11753	PLEK2	0.44902026	1.36511289	0.29798807	9.29110747	0.00016739	0.02863927
16822	UBA7	0.44037964	1.35696136	0.35566264	8.27797832	0.0003	0.04050646
16241	TNFSF10	0.43952497	1.35615771	0.19345632	18.8350193	4.22E-06	0.00214689
8655	LURAP1L	0.42782495	1.34520398	0.35430472	10.7707769	7.86E-05	0.01867561
15978	TMEM140	0.40603728	1.32504126	0.34596706	12.6281617	3.45E-05	0.00970443
14977	SQOR	0.40394429	1.32312035	1.05824899	8.67206446	0.00023738	0.0368287
8993	MDM2	0.39511882	1.31505106	4.56423622	7.88614591	0.00038239	0.04487469
817	APOL2	0.3887501	1.30925862	0.28051754	17.8266791	5.65E-06	0.00258527
5286	FAS	0.38374982	1.30472867	1.04283361	8.23867696	0.00030725	0.04059251
3910	DDA1	0.34606134	1.27108573	3.35988607	8.19079278	0.00031637	0.04082849
16498	TRIM56	0.3442917	1.26952755	0.85055072	10.3459483	9.66E-05	0.02083598
3920	DDIT3	0.33910742	1.26497372	0.1969755	13.846816	2.13E-05	0.00672484
10238	NOV	0.33675109	1.26290935	0.24475972	10.3320323	9.73E-05	0.02083598
5061	FAM129A	0.32785651	1.25514714	0.7110746	8.26089824	0.00030313	0.04050646
4079	DHRS9	0.3240847	1.25186995	1.69941514	9.58588295	0.00014277	0.02667082
1069	ASNS	0.32372788	1.25156036	0.58470597	9.31218999	0.00016547	0.02857813
8328	LGALS3BP	0.31026698	1.23993714	0.45913374	7.7414553	0.00041935	0.04889791
7451	IRF7	0.30652739	1.23672727	0.30310144	7.99396608	0.00035733	0.04361047
10178	NMI	0.28810312	1.22103378	1.62495265	7.69144385	0.00043308	0.04955274
5848	GALNT6	0.28689903	1.22001512	1.0005737	10.2931951	9.92E-05	0.02087049
6726	HIP1R	0.28007855	1.214261	0.66114255	8.58211409	0.0002502	0.03709546
806	APOBEC3G	0.27874604	1.21313999	0.29662742	9.04370114	0.00019198	0.0309825
4005	DEGS1	0.27717132	1.21181655	2.28429764	10.0696385	0.000111	0.02283314
10382	NT5C3A	0.26557897	1.20211838	0.54130752	9.52801709	0.00014725	0.02695697
818	APOL3	0.25871446	1.19641214	0.23136167	11.0161924	6.99E-05	0.01707096
10357	NSAP11	0.25256458	1.19132297	0.30111307	9.03485897	0.00019293	0.0309825
1765	C19orf44	0.22990501	1.17275773	0.41923689	8.15503803	0.00032338	0.04082849
15304	SWT1	0.22760185	1.170887	0.31086316	12.0478784	4.40E-05	0.01184452
5907	GBP5	0.22603437	1.16961553	0.16377252	13.2538818	2.68E-05	0.00790714
6654	HELZ2	0.21639753	1.16182883	0.23286018	8.17440358	0.00031956	0.04082849
5644	FOXF1	0.19968702	1.14844918	0.40771926	10.3981892	9.41E-05	0.02083598
6800	HLA-B	0.19831702	1.14735912	0.20320196	9.12096681	0.00018387	0.0300542
624	ANGPTL2	0.18237471	1.13475018	0.55269417	9.33044563	0.00016383	0.02857813
7548	JADE2	0.18146715	1.13403656	0.75448634	7.66288405	0.00044116	0.04985415
5840	GALNT12	0.15790543	1.11566619	0.25795642	8.60125311	0.00024741	0.03709546
950	ARL14	0.13147476	1.09541289	0.1746417	7.71282616	0.00042715	0.04944751

Table 3. List of down-regulated genes in response to a 4h-treatment with FXa over endothelial cells.

Differentially Expressed Genes of EA.hy926 treated cells							
36 Down regulated Coding Genes							
Row	**Symbol**	**logFC**	**FC**	**AveExpr**	**t**	**P.Value**	**adj.P.Val**
11235	PCDH10	-0.9371430	0.5222661	3.4010903	-9.2596691	0.0001703	0.0288673
7847	KIF20A	-0.7421827	0.5978342	3.0266095	-8.2833181	0.0002990	0.0405065
4629	EIF4B	-0.6510296	0.6368257	3.9516669	-31.4271420	0.0000003	0.0003183
878	ARHGAP18	-0.6046300	0.6576400	3.6994460	-8.2908197	0.0002977	0.0405065
16003	TMEM168	-0.5877096	0.6653984	1.1771837	-9.6813392	0.0001357	0.0261565
27	AASS	-0.5665095	0.6752485	1.7947316	-9.5664792	0.0001443	0.0266757
16306	TOP2B	-0.5585254	0.6789958	3.3181071	-8.0714223	0.0003405	0.0424057
10385	NT5DC2	-0.5144230	0.7000729	1.5054718	-8.0230257	0.0003509	0.0431141
15767	THBS1	-0.5118491	0.7013230	6.5664853	-13.2068813	0.0000273	0.0079272
11015	OSTF1	-0.4918005	0.7111370	3.7421444	-10.5226884	0.0000886	0.0202257
15030	SRSF7	-0.4693201	0.7223049	2.5975360	-7.7044442	0.0004295	0.0494475
6864	HNRNPA2B1	-0.4338687	0.7402740	2.3890562	-8.3102183	0.0002942	0.0405065
7743	KDM1A	-0.4288904	0.7428329	3.2887169	-13.6194635	0.0000232	0.0069722
4558	EFHD2	-0.3892041	0.7635507	1.5398818	-7.8864086	0.0003823	0.0448747
15420	TAF9B	-0.3890064	0.7636554	2.8660856	-7.9486572	0.0003676	0.0442761
4555	EFHC1	-0.3653463	0.7762825	2.1353800	-8.9604760	0.0002012	0.0320273
11540	PHKB	-0.3436562	0.7880417	2.5823831	-14.7010364	0.0000156	0.0052791
9091	METTL2A	-0.3434154	0.7881732	1.3761149	-8.0598215	0.0003430	0.0424234
6454	GTF2A1	-0.3366861	0.7918582	2.2970573	-7.9285195	0.0003723	0.0445473
3525	CS	-0.3312455	0.7948500	1.3603206	-8.0929090	0.0003360	0.0421319
6877	HNRNPM	-0.3304000	0.7953159	4.4900134	-11.5047413	0.0000559	0.0146160
9239	MLH1	-0.3144072	0.8041814	2.0125569	-11.4542018	0.0000572	0.0147422
5837	GALNT1	-0.3050064	0.8094386	4.2741418	-9.3832885	0.0001592	0.0282940
16609	TSN	-0.3007371	0.8118375	1.9215102	-8.1656399	0.0003213	0.0408285